

A multi-isotope (B, Sr, O, H, and C) and age dating (^3H – ^3He and ^{14}C) study of groundwater from Salinas Valley, California: Hydrochemistry, dynamics, and contamination processes

Avner Vengosh,¹ Jim Gill,² M. Lee Davisson,³ and G. Bryant Hudson⁴

Received 14 March 2001; revised 1 August 2001; accepted 6 September 2001; published 31 January 2002.

[1] The chemical and isotope ($^{11}\text{B}/^{10}\text{B}$, $^{87}\text{Sr}/^{86}\text{Sr}$, $^{18}\text{O}/^{16}\text{O}$, $^2\text{H}/\text{H}$, $^{13}\text{C}/^{12}\text{C}$, ^{14}C , and $^3\text{He}/^3\text{H}$) compositions of groundwater from the upper aquifer system of the Salinas Valley in coastal central California were investigated in order to delineate the origin and processes of groundwater contamination in this complex system. The Salinas Valley has a relatively deep, confined “400-foot” aquifer, overlain by a “180-foot” aquifer and a shallower perched aquifer, all made up of alluvial sand, gravel and clay deposits. Groundwater from the aquifers have different ^{14}C ages: fossil ($^{14}\text{C} = 21.3$ percent modern carbon (pmc) for the 400-foot aquifer and modern ($^{14}\text{C} = 72.2$ – 98.2 pmc) for the 180-foot aquifer. Fresh groundwater in all aquifers is recharged naturally and artificially through the Salinas River. The two modes of recharge can be distinguished chemically. We identified several different saline components with distinguishable chemical and isotopic fingerprints. (1) Saltwater intrusion in the northern basin has Cl concentrations up to 1700 mg/L, a Na/Cl ratio less than seawater, a marine Br/Cl ratio, a Ca/Cl ratio greater than seawater, $\delta^{11}\text{B}$ between +17 and +38‰ and $^{87}\text{Sr}/^{86}\text{Sr}$ between 0.7088 and 0.7096. Excess dissolved Ca, relative to the expected concentration for simple dilution of seawater, correlates with $^{87}\text{Sr}/^{86}\text{Sr}$ ratios, suggesting base exchange reaction with clay materials. (2) Agriculture return flow is high in NO_3 and SO_4 , with a $^{87}\text{Sr}/^{86}\text{Sr} = 0.7082$, $\delta^{11}\text{B} = 19$ ‰ and $\delta^{13}\text{C}$ between –23 and –17‰. The ^3H – ^3He ages (5–17 years) and ^{14}C data suggest vertical infiltration rates of irrigation water of 3–10 m/yr. (3) Nonmarine saline water in the southern part of the valley has high total dissolved solids up to 3800 mg/L, high SO_4 , Na/Cl ratio >1 , $\delta^{11}\text{B}$ between +24 and +30‰, and $^{87}\text{Sr}/^{86}\text{Sr} = 0.70852$. This groundwater may have acquired its geochemical signature from leaching of sedimentary rocks associated with the Coast Range marine deposits of Mesozoic to early Cenozoic age. The combination of different geochemical and isotopic fingerprints enables us to delineate the impact of salt sources in different areas of the valley and to reconstruct the origin of the SO_4 -enriched NO_3 -depleted saline plume that is located west of the city of Salinas. We suggest that the latter is derived from a mixture of different natural saline waters rather than from anthropogenic contamination. **INDEX TERMS:** 1040 Geochemistry: Isotopic composition/chemistry; 1045 Geochemistry: Low-temperature geochemistry; 1803 Hydrology: Anthropogenic effects; 1806 Hydrology: Chemistry of fresh water; **KEYWORDS:** coastal aquifer, salinization, geochemistry, isotope hydrology

1. Introduction

[2] Because world population centers tend to concentrate in coastal areas, groundwater sources in coastal aquifers are typically under stress due to overuse for domestic and agricultural consumption. Consequently, the quality of groundwater has been impacted by seawater intrusion, which further limits its future use. Salinization of groundwater is one of the main processes that affect groundwater quality in aquifers along the coast of California [Planert and Williams, 1995; Konikow and Rielly, 1999]. Saltwater intrusion occurs in many coastal aquifers in California including the Santa Ana basin in Orange County [Davisson *et al.*, 1999b],

Oxnard Plain in Ventura County [Izbicki, 1991], Salinas basin in Monterey County [Showalter *et al.*, 1984], and Capitola in Santa Cruz County [Essaid, 1999]. In general, overexploitation results in decrease of piezometric surfaces to below natural fresh-saline interface and subsequent intrusion of seawater into the pumping zones of the coastal aquifers. However, recent saltwater intrusion is not the only source of high salinity that affects the quality of groundwater. In addition, salinization can result from leakage of contaminated shallow aquifers through failed well casings, agriculture return flows, or upconing of underlying brines. Previous studies in the Salinas Valley [Showalter *et al.*, 1984; Heard, 1992; Todd, 1989; Staal, Gardner, and Dunne, Inc., 1993] showed that seawater intrusion is not the only source of salinity because other saline sources exist in the southern part of the basin.

[3] In this paper, we investigate the sources of the salinity in the 100-km-long Salinas Valley in central California (Figure 1). This aquifer is the principal source of $660 \times 10^6 \text{ m}^3/\text{yr}$ of groundwater that is mostly used for irrigation to support a multibillion dollar agricultural industry. The diversity of potential nonpoint salinity sources (e.g., seawater intrusion, agriculture return flows, connate saline water from poorly flushed aquifers, saline water entrapped in clay layers, and deep basin brines) requires diagnostic tools to delineate their origin and determine their impact on the ground-

¹Department of Geological and Environmental Sciences, Ben Gurion University of the Negev, Beer Sheva, Israel.

²Earth Sciences Department, University of California, Santa Cruz, California, USA.

³Health and Ecological Assessment Division, Lawrence Livermore National Laboratory, Livermore, California, USA.

⁴Analytical and Nuclear Chemistry Division, Lawrence Livermore National Laboratory, Livermore, California, USA.

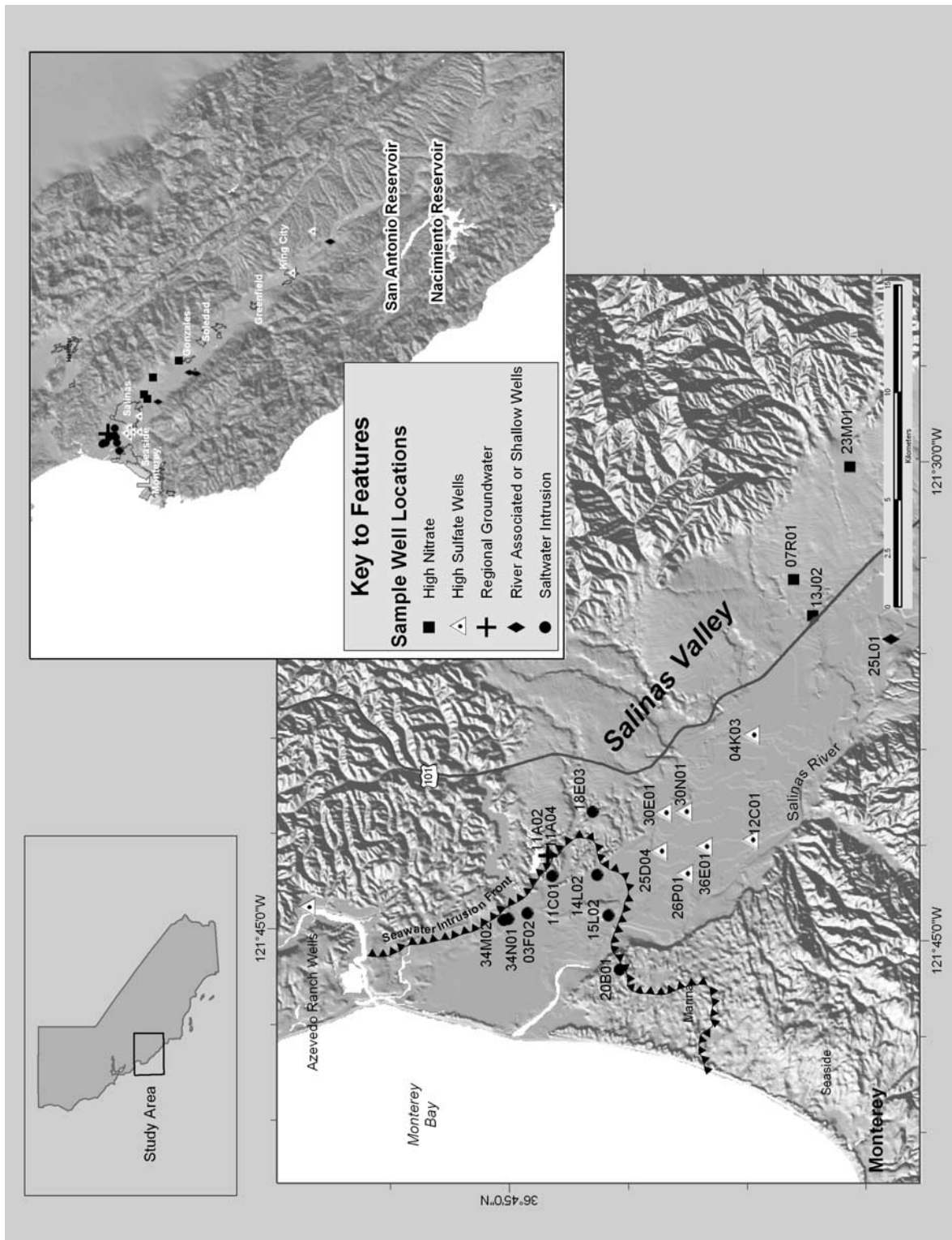


Figure 1. The Location maps for the samples studied at increasingly greater scales. Well locations are marked by symbols that denote the predominant chemical component. Well names are the final digits of the Monterey County Water Resources Agency (MCWRA) designations; the township/range prefixes are omitted. The sinusoidal hatched line shows the location in 1997 of the 500-mg/L isopleth contour and marks the “seawater intrusion front.”

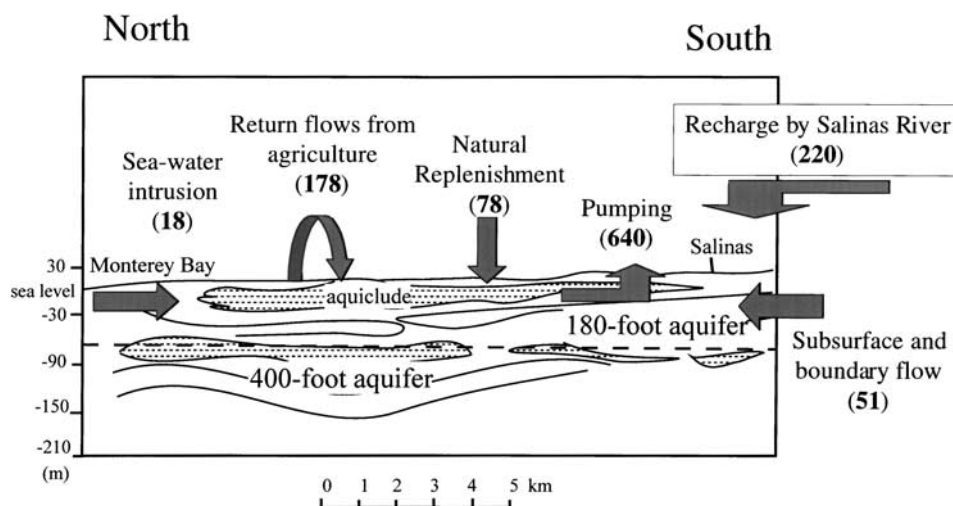


Figure 2. Schematic hydrogeological cross section of the Salinas Valley aquifer system and principle flow components of the basin. The hydrogeological cross section was modified from *Showalter et al.* [1984]. The numbers in parentheses are the estimated annual flow volume in 10^6 m^3 . Values for the flow components were taken from the *MCWRA* [1995] and their Web site (<http://www.mcwra.co.monterey.ca.us/>) Salinas Valley Integrated Ground and Surface Water Model Update of May 1997 (M. Watson, personal communication, 2000).

water system. We use conservative source and age indicators of water (Br/Cl , $\delta^{18}\text{O}$, $\delta^2\text{H}$, and $^3\text{H}-^3\text{He}$) and the isotopic composition of the dissolved constituents ($^{11}\text{B}/^{10}\text{B}$, $^{87}\text{Sr}/^{86}\text{Sr}$, ^{14}C , and $^{13}\text{C}/^{12}\text{C}$) in order to identify the salinity sources and evaluate the recharge regimes and flow rates of groundwater in the aquifer. We hypothesize that each of the salinity sources has a unique geochemical fingerprint that can be used to assess the relative impact of each component of groundwater quality. Even though the regional water agency (Monterey County Water Resources Agency) uses a 500-mg/L Cl isopleth to define the current (post 1950) “seawater intrusion front,” we show that this criterion can include nonseawater sources and exclude evidence for the most recent incursion.

2. Hydrogeological Setting

[4] The Salinas Valley groundwater basin (Figure 1) consists of four subareas (Pressure, East Side, Forebay, and Upper Valley) and two main water-bearing zones, the upper “180-foot” (55 m) and “400-foot” (122 m) aquifers which are separated by an impermeable clay layer at ~ 80 m that is up to 30 m thick (Figure 2). A perched aquifer overlies the 180-foot aquifer in the northern part of the valley above a clay layer that is usually, but not uniformly, present at a depth ≥ 15 m (the Salinas Valley Aquiclude). A deep lower aquifer system underlies the 400-foot aquifer. The 180-foot aquifer is up to 55 m thick. The perched and 180-foot aquifers consists of Pleistocene to Holocene gravels, sands, silts, and clays, which were deposited as alluvial/fluvial valley fill. The 400-foot aquifer lies at a depth of 82–143 m and is part of the Pleistocene Aromas and Pliocene Paso Robles formations. The aquifer consists of poorly bedded sands, gravels, volcanic tuff, and interbedded clays, which act as local aquitards. *Greene* [1970] showed that both the 180- and 400-foot aquifers crop out on the walls of Monterey Bay submarine canyon, which allows direct hydraulic connection between fresh and ocean water.

[5] The 100-km long Salinas Valley has been cultivated for over a century, with current annual pumping of $\sim 640 \times 10^6 \text{ m}^3/\text{yr}$ supplied predominantly from groundwater (see Monterey County Water Resources Agency, (MCWRA) at <http://www.mcwra.co.monterey.ca.us/>)(herein after referred to as MCWRA, web site) The 25–40

cm/yr of rainfall in the Salinas Valley does not sufficiently recharge aquifers with current groundwater demand, which far exceeds natural recharge rates (Figure 2). Therefore, because of decreasing water level conditions in the basin, the San Antonio and Lake Nacimiento Reservoirs were constructed in 1948 and 1957, respectively, to supplement irrigation requirements (Figure 1 top right) Annual average reservoir release is $\sim 324 \times 10^6 \text{ m}^3/\text{yr}$ to the Salinas River, which transports the releases to the Forebay and Pressure subareas in order to supplement recharge (*MCWRA*, web site). About two thirds of the release is recharged, and the rest flows to the ocean. The reservoirs have supplemented groundwater demand and brought the basin close to hydrologic balance. Seawater intrusion has been a chronic problem for >50 years. In the 180-foot aquifer the current “seawater intrusion front,” defined as the 500-mg/L Cl contour, lies ~ 10 km inland, between the cities of Castroville and Salinas (Figure 1). The overall hydrological balance of the Salinas basin (*MCWRA*, web site) is presented schematically in Figure 2. The objective of this study is to characterize the chemical and isotopic compositions of each of the input components and to examine their overall impacts on the water quality in the basin.

3. Methods and Analytical Techniques

[6] Between fall of 1996 and summer of 1997, 46 representative samples from 37 different locations were collected from irrigation and monitoring wells and surface waters in the Salinas Valley. Water samples were collected using ultraclean acid-washed bottles for Sr isotopes, glass bottles with air-tight caps for ^3H and ^{14}C (HgCl_2 added as preservative), and copper tubes with pinch clamps for noble gas analysis. Analyses of major ions were performed at the Monterey County Chemistry Laboratory. B and Li concentrations were measured by inductively coupled plasma–mass spectrometer (Element, Finnigan) at the University of California, Santa Cruz. The ^{11}B and ^7Li intensities were normalized to a ^9Be internal standard. Spike-free samples were scanned before the analyses, and no detectable levels of ^9Be were found in the original samples. Br was determined by flow injection ion analyzer (QuickChem 8000) at the Hydrological Service laboratory in Jerusalem [*Vengosh and Pankratov*, 1998].

Table 1. Chemical and Isotopic Compositions of Groundwater and Surface Water From Salinas Valley, California^a

Well	Aquifer/Site	Well Depth, m	Screen Interval, m	Date ^b	T	pH	Ca	Mg	Na	K	Li	Sr	Cl	Br	SO ₄	HCO ₃	NO ₃	B	$\delta^{18}\text{O}$, ‰	δD , ‰	$\delta^{13}\text{C}$, ‰	$\delta^{11}\text{B}$, ‰	$^{87}\text{Sr}/^{86}\text{Sr}$	^{14}C (PMC)		
<i>Ground Fresh Water</i>																										
Northern basin																										
14S/2E-11A2 ^c	180 feet (northern basin)	76.2	57.9–73.1	21/1/1997	20	7.7	48	14	32	2.3	0.0056	0.241	28	0.09	5	203	1	0.035	-6.13				16.8	0.709008		
14S/2E-11A2 ^c	180 feet (northern basin)	76.2	57.9–73.1	7/7/1997	20.5	46	14	28	2.1	0.0046	0.278	25	0.15	8	202	3	0.029	-6.53	-43.2	-13.1	18.4	0.709001				
14S/2E-11A4 ^e	400 feet deep	149.4	137.2–146.3	21/1/1997	22	7.6	43	13	41	3	0.0171	0.271	37	0.05	9	187	3	0.049	-6.30			7.5	0.708990			
14S/2E-11A4 ^e	400 feet deep	149.4	137.2–146.3	7/7/1997	22.6	39	12	36	2.2	0.0154	0.271	32	0.15	9	178	3	0.048	-6.30	-44.4	-13.7		0.708991	21.3			
Southern basin																										
17S/4E-1D1 ^d	180 feet (southern basin)	94.5		9/7/1997	18.7	7.4	94	30	32	3.1	0.0080	0.525	27	0.2	148	228	6	0.115	-5.36	-38.5	-13.0		0.710080			
15S/3E-25L1 ^d	180 feet (southern basin)	119.5	40.5–46.3	9/7/1997	17.1	7.5	88	31	37	3.4	0.0081	0.516	27	0.24	139	220	12	0.152	-4.96	-37.8	-13.1	22.9	0.709655			
16S/4E-25Q1 ^d	180 feet (southern basin)			9/7/1997	17.4	7.1	72	27	56	3	0.0071	0.446	30	0.12	118	222	0	0.169	-4.89	-37.4	-12.6		0.709288			
21S/9E-21T52 ^d	shallow (southern basin)	30.5	15.2–27.4	13/6/1997	17.3						0.0121		61		130		3	0.265	-5.40	-42.0			0.709001			
(San Lucas 4)																										
21S/9E-21T51 ^d	shallow (southern basin)	30.5	15.2–27.4	13/6/1997	18.4	69	26	67	2.1	0.0138		124			123	169	1	0.477	-5.50	-44.7			0.709053			
(San Lucas 5)																										
<i>Surface Water</i>																										
Lake Nacimiento	lake water			15/5/1997			21	24	7	1	0.0034		1		24	81	1	0.026					0.708902			
Lake Nacimiento	outflow below dam			13/6/1997	11.9						1.008		4		31		1		-6.23	-41.7			0.708870			
Lake San Antonio	lake water			15/5/1997			29	12	12	2	0.0038		7		49	87	3	0.020					0.710165			
Lake San Antonio	outflow below dam			13/6/1997	14						1.048		11		56		1	0.020	-5.42	-43.0			0.710192			
Lake San Antonio	down stream			13/6/1997	17.5								8		54		1		-5.46	-43.6			0.710233			
Salinas River	San Lucas Bridge			13/6/1997	23.5						0.0048		13		51		1	0.081	-5.77	-43.5			0.709059			
Salinas River	San Ardo Bridge			13/6/1997	23						0.0038		7		44		0	0.037	-5.88	-41.7			0.709059			
Salinas River	Gonzales River Bridge			9/7/1997	26.5	8.3	40	16	19	2.1	0.0062	0.276	16		67	120	3	0.085	-4.70	-35.5	14.5		0.709078			

Table 1. (continued)

Well	Aquifer/Site	Well Depth, m	Screen Interval, m	Date ^b	T	pH	Ca	Mg	Na	K	Li	Sr	Cl	Br	SO ₄	HCO ₃	NO ₃	B	δ ¹⁸ O, ‰	δD, ‰	δ ¹³ C, ‰	δ ¹¹ B, ‰	⁸⁷ Sr/ ⁸⁶ Sr	¹⁴ C (PMC)	
<i>Saltwater Intrusion</i>																									
14S/2E-20B1 ^d	400 feet	106.7	79.2-103.6	31/1/1997		392	124	470	11.2		2.268	1702		214	63	40								0.709634	
14S/2E-20B1 ^d	400 feet	106.7	79.2-103.6	5/11/1996	19.5	7.2	410	126	450	11.6	0.0257	2.315	1670	5.35	212	62	40	0.203	-6.02					0.709535	
14S/2E-15L2 ^d	180 feet	61.3	45.1-59.4	7/7/1997	17.8	7.4	309	105	193	9.4	0.0316	2.045	973	3.44	141	148	1	0.245	-6.60	-44.7				0.709262	
13S/2E-34M2 ^d	180 feet			5/11/1996	16.5	7.0	273	89	118	5.4	0.0290	0.859	726	2.06	113	205	30	0.119	-6.24					0.708760	
14S/2E-14L2 ^d	180 feet	38.1		5/11/1996	19.5	7.5	217	82	98	5.8	0.0285	1.153	650	2.12	58	142	3	0.104	-6.58					0.708997	
14S/3E-18E3 ^b	260 feet shallow	79.2	70.1-76.2	21/1/1997	19	7.3	126	48	109	2.8	0.0209	0.936	389	0.83	17	166	1	0.097	-5.72					0.708714	93.4
14S/2E-11C1 ^d	180 feet	67.1	50.3-67.1	8/7/1997	20.5	6.9	303	105	136	5.7	0.0214		593	1.22	206	398	186	0.146	-5.69	-43.6	-17.4	38.2		0.709210	
13S/2E-34N1 ^d	180 feet			5/11/1996	15.5	7.3	219	93	144	5.8	0.0271	1.117	400	0.93	230	399	154	0.139	-5.69					0.709013	
14S/2E-03F2 ^d	180 feet	35.7	28.6-35.7	4/11/1996	18	7.2	168	75	260	5.9	0.0276	1.001	254	0.68	158	393	447	0.260	-5.31					0.708945	
<i>High Nitrate</i>																									
14S/2E-11A3 ^c	100 feet, perched	30.5	18.3-27.4	21/1/1997	18.5	6.8	107	61	78	2.5	0.0127	0.959	118	0.28	299	205	53	0.194	-6.49					0.708207	85.1
14S/2E-11A3 ^c	100 feet, perched	30.5	18.3-27.4	7/7/1997	18.9	110	56	76	2.4	0.0146	0.808		156	0.31	262	208	53	0.216	-6.21	-42.6	-20.1	19.0		0.708199	
15S/3E-13J2 ^d	180 feet	115.8	108.5-115.8	9/7/1997	17.4	7	104	53	101	3.5	0.0163		150	0.46	135	284	97	0.238	-6.3					0.708951	98.4
15S/4E-23M1 ^d	180 feet			8/7/1997	18.7	6.9	70	38	71	2.1	0.0171	0.454	115	0.7	56	96	218	0.035	-6.08	-44.9	-23.5	33.8		0.709674	72.2
15S/4E-7R1 ^d	180 feet	53.3		20/5/1997	19	7.3	103	44	139	4	0.0169	0.661	125	0.42	126	139	457	0.095	-5.75	-42.3				0.709312	
Azevedo top ^c	perched			2/5/1997	18.9	6.4	107	49	69	10	0.0081	0.916	113	5.73	301	37	239	0.095	-5.69	-40.8				0.707634	
Azevedo middle ^c	perched			2/5/1997	18	6.1	91	48	70	4.8	0.0080	0.78	114	5.22	271	15	199	0.076	-5.56	-39.0				0.707540	
Azevedo bottom ^c	perched			2/5/1997	17	6.2	143	57	68	11.6	0.0027	1.294	163	2.69	343	13	311	0.140	-5.50	-39.4				0.707678	
<i>South Valley</i>																									
20S/8E-5R3 ^d	180 feet	106.7		10/4/1997	19	7.2	140	58	250	4.8	0.0784	1.474	285	0.97	415	279	39	1.220	-5.61	-44.7				0.708831	
20S/9E-26N1 ^d	30 feet	96.3	57.3-88.4	10/4/1997	25	6.9	372	206	500	27	0.4954		558	2.46	1929	163	1	1.680	-5.95	-51.1				0.708524	
Carter Ranch 1 ^d (San Lucas)	60 feet			10/4/1997	19.5	7.4	411	117	500	24	0.3748	2.67	549	2.22	1716	145	38	1.711	-5.94	-49.3				0.708398	
<i>Banana Belt</i>																									
14S/2E-26P1 ^c	180 feet			20/5/1997	21	7.1	226	80	113	5	0.0015	1.437	345	1	386	275	3	0.170	-6.72	-48.8				0.709394	
14S/2E-26D4 ^c	180 feet	25.9		4/11/1996	18	7.3	213	74	141	6.3	0.0281	1.168	316	1.05	371	373	3	0.349	-6.29					0.708937	
14S/3E-30E1 ^c	180 feet			20/5/1997	20.4	7.1	156	61	200	5	0.0019	0.904	238	0.6	357	365	73	0.407	-5.77	-42.7				0.709010	
14S/3E-30N1 ^c	180 feet	62.5		21/5/1997	20.5	7.6	166	64	170	6	0.0021	1.008	190	0.78	372	366	98	0.426	-5.88	-44.5				0.708915	
14S/2E-36E1 ^c	180 feet	60.4		9/7/1997	19.4	7.0	189	56	133	7.6	0.0194	1.048	164	0.66	457	374	4	0.423	-6.35	-45.4	-15.1	33.4		0.710001	84.0
15S/2E-12C1 ^c	180 feet	55.5		20/5/1997	19	7.4	140	47	91	5	0.0015	0.919	128	0.47	307	304	23	0.234	-6.26	-43.7				0.709803	
16S/5E-3C1 ^c	180 feet	102.1		10/4/1997	17.5	7.8	113	42	70	3	0.0147	0.665	48	0.17	267	288	13	0.238	-5.77	-44.8				0.709002	
15S/3E-04K3 ^c	400 feet			4/11/1997	19.5	7.7	88	27	64	4.1	0.0166	0.477	41	0.19	179	235	1	0.184	-6.17					0.709231	

^a Chemical units are given in mg/L.
^b Date format is day, month, year.
^c Monitoring well is indicated.
^d Production well is indicated.

[7] Boron isotopes were measured by negative thermal ionization mass spectrometry [Vengosh *et al.*, 1989, 1994]. Samples were analyzed by a direct loading procedure in which boron-free seawater and natural solutions were loaded directly onto Re filaments and measured in a reverse polarity National Bureau of Standards (NBS) style 12-inch solid-source mass spectrometer at the University of California, Santa Cruz. A standard deviation of <1.5‰ was determined by repeat analysis of National Institute of Standards and Technology SRM-951 standards ($^{11}\text{B}/^{10}\text{B}=4.013\pm 0.005$). Isotope ratios are reported as $\delta^{11}\text{B}$ values, where $\delta^{11}\text{B}=[((^{11}\text{B}/^{10}\text{B})_{\text{sample}}/ (^{11}\text{B}/^{10}\text{B})_{\text{NBS951}})-1]1000$.

[8] Strontium was separated by cation exchange chromatography using standard techniques. Isotope ratios were determined using third-generation Faraday detectors in static mode on a VG-54WARP mass spectrometer at University of California, Santa Cruz. Zone refined rhenium filaments were used on all samples. All measured $^{87}\text{Sr}/^{86}\text{Sr}$ ratio of 0.1194 using an exponential correction law. Correction for ^{87}Rb was negligible for all samples. Using this procedure, the NBS-987 standard yielded a $^{87}\text{Sr}/^{86}\text{Sr}$ ratio of 0.71025 (± 0.00001 , $n = 5$) during the period in which the unknowns were run.

[9] The ^{18}O and deuterium were analyzed respectively by using the CO_2 equilibration [Epstein and Mayeda, 1953] and the zinc reduction methods [Coleman *et al.*, 1982], followed by isotopic measurements. All stable isotope data are reported in the usual δ notation, where $\delta = (R/R_{\text{STD}} - 1)1000$, R represents either the $^{18}\text{O}/^{16}\text{O}$, D/H , or $^{13}\text{C}/^{12}\text{C}$ ratio of the sample, and R_{STD} is the isotope ratio of the standard mean ocean water or peedee belemnite standard. The ^3H was analyzed by the helium accumulation method [Surano *et al.*, 1992], where samples are cryogenically degassed, sealed, and stored for 15–60 days to allow accumulation of ^3He from the tritium decay. The sample was subsequently degassed, and the ^3He was isolated and measured on a VG-5400 noble gas mass spectrometer. Copper tubes for dissolved noble gas analysis held air-free samples that were vacuum fitted to an evacuated container, the pinch clamp and copper seal was uncrimped, and the water sample was released. The water was degassed, and the noble gases of interest were isolated and analyzed [Schlosser *et al.*, 1988].

[10] The inorganic carbon was acid stripped under high vacuum and purged with an ultrapure carrier gas [Davisson and Velsko, 1994; McNichol *et al.*, 1994]. Liberated CO_2 was reduced to graphite [Vogel *et al.*, 1987], and all ^{14}C concentrations were determined using the accelerator mass spectrometer at Lawrence Livermore National Laboratory. The ^{14}C results are reported as a percent modern carbon (pmc) relative to a NBS oxalic acid standard [Stuiver and Polack, 1977]. CO_2 was split for $\delta^{13}\text{C}$ analysis on an isotope ratio mass spectrometer.

4. Results and Discussion

[11] Chemical and isotopic (B, Sr, O, H, and C) results are presented in Table 1, whereas ionic ratios are reported in Table 2. The ^{14}C and $^3\text{He}/^3\text{H}$ results are reported in Table 3. We distinguish between different groundwater types (Figure 3): (1) fresh groundwater (total dissolved solids (TDS) <500 mg/L) in both the 180-foot and 400-foot aquifers in the north and surface water plus shallow groundwater closely associated with recharge from the Salinas River in the south; (2) saltwater intrusion affected groundwater in the north; (3) nitrate-rich groundwater from the shallow perched aquifer with high concentrations of nitrate (up to 460 mg/L) and sulfate (up to 340 mg/L); and (4) sulfate-rich groundwater (TDS up to 3800 mg/L) in the central and southern parts of the

valley. The chemical, $\delta^{18}\text{O}$, $\delta^{11}\text{B}$, and $^{87}\text{Sr}/^{86}\text{Sr}$ variations are presented in Figures 3, 4, 5, and 6.

4.1. Freshwater Components

[12] We examined two sets of fresh water in order to evaluate the chemical and isotopic compositions of the freshwater component: (1) uncontaminated groundwater from the 180- and 400-foot aquifers from the Pressure area in the north and (2) surface water plus shallow and 180-foot groundwater from the southern and central parts of the valley (Tables 1 and 2).

[13] The freshest groundwater in our study comes from research wells in the 180-foot and 400-foot aquifers in the north (14S/2E-11A2 and 14S/EE 14S/EE-11A4, respectively, (Figure 1)). These wells are adjacent to a detention pond (Espinosa Lake) and <150 m from the 1995 seawater intrusion front in the 180-foot aquifer. We consider them to be most representative of local meteoric recharge and will refer to them hereafter as “fresh groundwater.”

[14] Fresh groundwater recharge in the southern valley is also affected by waters held in the two reservoirs and released via the Salinas River. These waters differ chemically from direct meteoric recharge by having higher SO_4 , B, and Li relative to C1 (Tables 1 and 2), reflecting their passage through the soils and rocks of the Santa Lucia Mountains bordering the Salinas Valley to the west.

[15] In addition, water in the two reservoirs in the Santa Lucia Mountains that feed the Salinas River differs isotopically. Lake San Antonio water has $^{87}\text{Sr}/^{86}\text{Sr}$ of ~ 0.710026 , $\delta^{18}\text{O}$ of -5.4 , and δD of -44 , whereas the same parameters in Lake Nacimiento waters are 0.708852, -6.2 , and -42 , respectively. The difference in Sr reflects the contrasting lithologies of their respective drainages. The Lake San Antonio drainage lies entirely within the Salinian Block that contains radiogenic Cretaceous S-type granites and Miocene continental shelf sediments, whereas the Lake Nacimiento drainage also includes Franciscan mafic and ultramafic rocks. The difference indicates that Sr isotopes have equilibrated quickly through cation exchange with the surrounding bedrock [e.g., Johnson and DePaolo, 1994] during infiltration flow.

[16] Reasons for the difference in $\delta^{18}\text{O}$ and δD are more complex. Lake San Antonio has more surface area which may explain the more evaporated character of the water. After correcting for evaporation using a slope of 5, Lake San Antonio waters intersect the Global Meteoric Water Line at substantially lighter values, suggesting rainfall at higher elevations even though the Lake Nacimiento drainage also includes high mountains.

[17] The Salinas River has appropriately intermediate values of all isotope ratios (Table 1). Its $^{87}\text{Sr}/^{86}\text{Sr}$ ratio of 0.709078 suggests a mixing proportion of 15% San Antonio and 85% Nacimiento which was the respective reservoir discharge rate in the weeks preceding sample collection (K. Thomasberg, MCWRA, personal communication, 2000).

[18] Five wells in the vicinity of the Salinas River are listed under “fresh water” in Table 1 and show a range in $^{87}\text{Sr}/^{86}\text{Sr}$ ratios (0.70900–0.71008) that is within the range of the surface waters. All have $\delta^{18}\text{O}$ values intermediate between San Antonio Reservoir and Salinas River water and show distinct evaporative stable isotope signatures, generally lying along the evaporation trajectory of the Salinas River (Figure 4a). They are the isotopically heaviest groundwater samples we studied and the most likely to have been directly recharged by the river.

4.2. Seawater Intrusion

[19] Saline waters associated with modern seawater intrusion into the Pressure area of the northern section of the Salinas Valley

Table 2. Ionic Ratios of Different Groundwater and Surface Water From Salinas Valley^a

Well	Aquifer/Site	Cl	Na/Cl	Ca/(SO ₄ + HCO ₃)	Mg/Cl	Ca/Cl	K/Cl	Li/Cl	SO ₄ / Cl	Br/Cl (×10 ⁻³)	B/Cl (×10 ⁻³)	NO ₃ /Cl
<i>Ground Fresh Water</i>												
<i>Northern basin</i>												
14S/2E-11A2	180 feet (northern basin)	28	1.76	0.70	0.73	1.52	0.074	0.0010	0.07	1.43	4.10	0.020
14S/2E-11A2	180 feet (northern basin)	25	1.73	0.66	0.82	1.63	0.076	0.0009	0.12	2.66	3.82	0.069
14S/2E-11A4	400 feet deep	37	1.71	0.66	0.51	1.03	0.074	0.0024	0.09	0.60	4.34	0.046
14S/2E-11A4	400 feet deep	32	1.73	0.63	0.55	1.08	0.062	0.0025	0.10	2.08	4.97	0.054
<i>Southern basin</i>												
17S/4E-1D1	180 feet (southern basin)	27	1.83	1.26	1.62	3.08	0.104	0.0015	2.02	3.29	13.9	0.127
15S/3E-25L1	180 feet (southern basin)	27	2.11	1.22	1.67	2.89	0.114	0.0015	1.90	3.94	18.5	0.254
16S/4E-25Q1	180 feet (southern basin)	30	2.88	0.99	1.31	2.12	0.091	0.0012	1.45	1.77	18.5	
21S/9E-21T52(San Lucas 4)	shallow (southern basin)	61						0.0010	0.79		14.2	0.028
21S/9E-21T51(San Lucas 5)	shallow (southern basin)	124	0.83	1.24	0.31	0.49	0.015	0.0006	0.37		12.6	0.005
<i>Surface Water</i>												
Lake Nacimiento	lake water	1	10.80	0.79	35.01	18.59	0.907	0.0172	8.86		84.5	0.572
Lake Nacimiento	outflow below dam	4							2.86			0.143
Lake San Antonio	lake water	7	2.64	1.02	2.50	3.67	0.259	0.0028	2.58		9.6	0.245
Lake San Antonio	outflow below dam	11							1.88			0.052
Lake San Antonio	down stream	8							2.49			0.071
Salinas River	San Lucas Bridge	13						0.0019	1.45		20.4	0.044
Salinas River	San Ardo Bridge	7						0.0019	1.45		20.4	0.044
Salinas River	Gonzales River Bridge	16	1.83	1.02	1.46	2.21	0.119	0.0020	1.55		17.4	0.107
<i>Saltwater Intrusion</i>												
14S/2E-20B1	400 feet	1702	0.43	3.57	0.11	0.20	0.006	0.0000	0.05			0.013
14S/2E-20B1	400 feet	1670	0.42	3.77	0.11	0.22	0.006	0.0001	0.05	1.42	0.39	0.014
14S/2E-15L2	180 feet	973	0.31	2.88	0.16	0.28	0.009	0.0002	0.05	1.57	0.83	0.001
13S/2E-34M2	180 feet	726	0.25	2.39	0.18	0.33	0.007	0.0002	0.06	1.26	0.54	0.024
14S/2E-14L2	180 feet	650	0.23	3.07	0.18	0.30	0.008	0.0002	0.03	1.45	0.52	0.003
14S/3E-18E3	260 feet, shallow	389	0.43	2.05	0.18	0.29	0.007	0.0003	0.02	0.95	0.81	0.001
14S/2E-11C1	180 feet	593	0.35	1.40	0.26	0.45	0.009	0.0002	0.13	0.91	0.81	0.179
13S/2E-34N1	180 feet	400	0.56	0.97	0.34	0.48	0.013	0.0003	0.21	1.03	1.14	0.220
14S/2E-03F2	180 feet	254	1.58	0.86	0.43	0.59	0.021	0.0006	0.23	1.19	3.36	1.006
<i>High Nitrate</i>												
14S/2E-11A3	100 feet, perched	118	1.02	0.56	0.75	0.80	0.019	0.0005	0.94	1.05	5.39	0.257
14S/2E-11A3	100 feet, perched	156	0.75	0.62	0.52	0.62	0.014	0.0005	0.62	0.88	4.54	0.194
15S/3E-13J2	180 feet	150	1.04	0.70	0.52	0.61	0.021	0.0006	0.33	1.36	5.19	0.370
15S/4E-23M1	180 feet	115	0.95	1.28	0.48	0.54	0.017	0.0008	0.18	2.70	0.98	1.084
15S/4E-7R1	180 feet	125	1.71	1.05	0.51	0.73	0.029	0.0007	0.37	1.49	2.50	2.091
Azevedo top	perched	113	0.94	0.78	0.63	0.84	0.080	0.0004	0.98	22.5	2.76	1.209
Azevedo middle	perched	114	0.95	0.77	0.61	0.71	0.038	0.0004	0.88	20.3	2.19	0.998
Azevedo bottom	perched	163	0.64	0.97	0.51	0.78	0.065	0.0001	0.78	7.32	2.82	1.091
<i>High Sulfate South Valley</i>												
20S/8E-5R3	180 feet	285	1.35	0.53	0.30	0.43	0.015	0.0014	0.54	1.51	14.0	0.078
20S/9E-26N1	30 feet	558	1.38	0.43	0.54	0.59	0.044	0.0045	1.28	1.96	9.87	0.001
Carter Ranch 1 (San Lucas)	60 feet	549	1.40	0.54	0.31	0.66	0.040	0.0035	1.15	1.79	10.2	0.040
<i>Banana Belt</i>												
14S/2E-26P1	180 feet	345	0.51	0.90	0.34	0.58	0.013	0.0000	0.41	1.29	1.62	0.005
14S/2E-25D4	180 feet	316	0.69	0.77	0.34	0.60	0.018	0.0005	0.43	1.47	3.62	0.005
14S/3E-30E1	180 feet	238	1.30	0.58	0.37	0.58	0.019	0.0000	0.55	1.12	5.61	0.175
14S/3E-30N1	180 feet	190	1.38	0.60	0.49	0.77	0.029	0.0001	0.72	1.82	7.34	0.295
14S/2E-36E1	180 feet	164	1.25	0.60	0.50	1.02	0.042	0.0006	1.03	1.79	8.45	0.014
15S/2E-12C1	180 feet	128	1.10	0.61	0.54	0.97	0.035	0.0001	0.89	1.63	5.99	0.103
16S/5E-3C1	180 feet	48	2.25	0.55	1.28	2.08	0.057	0.0016	2.05	1.57	16.3	0.155
15S/3E-04K3	400 feet	41	2.41	0.58	0.96	1.90	0.091	0.0021	1.61	2.06	14.7	0.014

^aRatios are given in equivalent units.

(Figure 1) have a Ca-chloride composition (i.e., Ca/(SO₄ + HCO₃) > 1) with high Cl/TDS (0.3–0.5), low Na/Cl (lower than the marine ratio of 0.86), and marine Br/Cl (1.5 × 10⁻³) ratios. On the basis of Cl concentration the most saline well available for sampling, 14S/2E20B1, was ~9% seawater. The good correlation between the conservative ions Br and Cl, and their marine ratio (Figure 3), supports a seawater intrusion source for these waters.

[20] All but one of our seawater intrusion samples (14S/3E-18E3) lie seaward of the recent “seawater intrusion front” as defined by the regional water agency (Figure 1). These waters have a distinctive chemical composition (e.g., lower SO₄ and B and higher Ca, relative to other water types at similar Cl concentration) that enables discrimination of early arrival of seawater intrusion from other saline waters. This distinction is traceable even at

Table 3. Noble Gas, ^3He , ^4He Data and Calculated Ages, Radiogenic Helium, and Excess Air

Well	^4He , atm/g $^3\text{He}/^4\text{He}$, at/at $(\times 10^{-6})$	Ne, atm/g Ar, atm/g $^4\text{He}_{\text{rad}}$, atm/g ^3H , pCi/L $(\times 10^{11})$	Via Ne, $\text{cm}^3\text{STP/g}$	trit ^3He , atm/g $(\times 10^5)$	Plus/Minus, ^3He , atm/g $(\times 10^5)$	Plus/Minus, $^3\text{H}-^3\text{He}$ age, years $(\times 10^4)$	Plus/Minus, $^3\text{H}-^3\text{He}$ age, years	pCi/L, Initial ^3H , at/at	$^4\text{He}/\text{Ne}$, at/at	Ar/Ne, at/at $(\times 10^3)$						
14S/02E-11A02	2.18	1.32	8.40	1.27	1.14	10.0	0.0063	0.45	0.58	2.10	2.34	3.5	4.1	12.2	2.6	1.52
14S/02E-11A03	1.72	1.40	7.28	1.15	-0.54	7.2	0.0040	0.59	0.48	1.51	2.22	5.9	4.2	10.0	2.36	1.58
14S/02E-36E01	1.54	1.28	4.93	0.94	4.14	3.8	-0.0008	5.90	0.39	7.94	2.13	38.2	4.4	32.0	3.13	1.91
15S/04E-23M01	4.54	1.41	1.72	1.72	-0.80	7.3	0.0242	1.31	1.28	1.52	2.22	11.1	8.2	13.5	2.64	1.00
16S/04E-25Q01	1.71	1.49	7.33	1.12	-0.86	12.6	0.0041	2.03	0.51	2.63	2.47	10.2	2.1	22.3	2.34	1.53
14S/02E-11C01	1.75	1.39	6.88	1.11	0.88	7.3	0.0032	1.80	0.49	1.52	2.22	14.0	3.0	15.9	2.54	1.62
17S/02E-01D01	1.65	1.69	6.14	0.99	1.73	19.0	0.0017	8.62	0.56	3.97	2.88	20.7	1.2	60.2	2.70	1.63
15S/03E-13J02	1.66	1.47	6.88	1.15	0.07	5.8	0.0032	1.84	0.49	1.20	2.17	16.6	3.5	14.6	2.41	1.67
15S/03E-25L01	2.18	1.43	8.85	1.24	-0.49	17.3	0.0072	1.33	0.62	3.62	2.77	5.6	2.3	23.7	2.46	1.40

concentrations <500 mg/L Cl, a threshold not reached by three of our samples, which lie seaward of the front.

[21] Seawater intrusion groundwater is enriched in Ca, Mg, Li, and Sr and is depleted in Na relative to diluted seawater with similar salinity (Table 2 and Figure 3). In addition, the groundwater, shows a wide range of SO_4/Cl ratios (0.02–0.23) relative to seawater (0.05). These changes indicate that water-rock interactions and sulfate reduction modified the original seawater. The possible water-rock modifications are (1) base exchange reactions, (2) dolomitization, and (3) diagenetic transformation of carbonate minerals [Jones *et al.*, 1999]. Assuming that seawater is the original water (i.e., it has a marine Br/Cl ratio) and that Cl is conservative, we can test whether the apparent Na depletion and Ca enrichment is due to Na in the water replacing Ca and Mg in sorbed sites on clay minerals. We use the marine Ca/Cl and Na/Cl ratios to calculate the expected concentrations of these elements in diluted seawater as defined by the Cl concentrations. The difference (Δ) between the measured and calculated Ca (and Na) is

$$\Delta\text{Ca} = [\text{Ca}]_{\text{meas}} - (\text{Ca}/\text{Cl})_{\text{SW}} [\text{Cl}]_{\text{meas}}. \quad (1)$$

As illustrated in Figure 6, the values of ΔCa have an inverse linear correlation with ΔNa (slope of -1), indicating a similar magnitude of Ca enrichment and Na depletion. This stoichiometry is consistent with a base exchange reaction [e.g., Appelo and Postma, 1993; Custodio *et al.*, 1987; Jones *et al.*, 1999].

[22] Sr and Ca concentrations correlate positively with $^{87}\text{Sr}/^{86}\text{Sr}$ ratios (Figure 6). These relationships suggest that (1) the marine Ca concentration and Sr isotopic ratio ($^{87}\text{Sr}/^{86}\text{Sr}$ of ~ 0.7092) were modified by base exchange reactions and (2) the modified Sr- and Ca-enriched groundwater was subsequently diluted by mixing with less radiogenic regional groundwater. Exchangeable Sr on clay minerals has a high $^{87}\text{Sr}/^{86}\text{Sr}$ ratio, ranging from 0.7103 to 0.7280 [Bullen *et al.*, 1997; Chaudhuri and Brookins, 1979; Chaudhuri *et al.*, 1987; Stueber *et al.*, 1987; Johnson and DePaolo, 1994]. Thus the increase of $^{87}\text{Sr}/^{86}\text{Sr}$ ratios over seawater in the intrusion area suggests that base exchange reactions add radiogenic Sr from the clay minerals. In contrast, Starinsky *et al.* [1983] demonstrated that during dolomitization reactions the $^{87}\text{Sr}/^{86}\text{Sr}$ ratio of the residuals fluids gradually decrease toward lower $^{87}\text{Sr}/^{86}\text{Sr}$ ratios that are typical of marine carbonates of ages from Cretaceous to recent. One would expect that recrystallization or dolomitization of Miocene sediments in the Salinas Valley (e.g., Monterey formation) would result in Ca-enriched water with $^{87}\text{Sr}/^{86}\text{Sr}$ ratios, which are lower than in modern seawater (i.e., <0.7092). However, it is likely that the aquifer sediments are dominated by siliclastic deposits and that carbonate minerals are not readily available for dolomitization reactions. This distinction should be further tested but potentially can provide an important geochemical tool to trace the origin of saline water and, in particular, to distinguish the effect of base exchange from dolomitization in the formation of Ca-enriched saline water.

[23] We observed apparent conservative mixing phenomena for reactive elements like Ca and Sr, but these elements are significantly enriched relative to seawater (as normalized to Cl). This shows that base exchange reactions occur only at the early stages of the evolution of seawater intrusion. It is possible that reaction ceases once the adsorbed sites become saturated with respect to Na, and further intrusion and mixing with local groundwater (in our case agriculture return flow) does not involve further base exchange reactions.

[24] The $\delta^{11}\text{B}$ values range from +12 to 38‰ in the most saline water, which suggests conservative mixing between seawater ($\delta^{11}\text{B} = +39$ [Spivack *et al.*, 1987]) and fresh water (+7.5 to +18) (Figure 5).

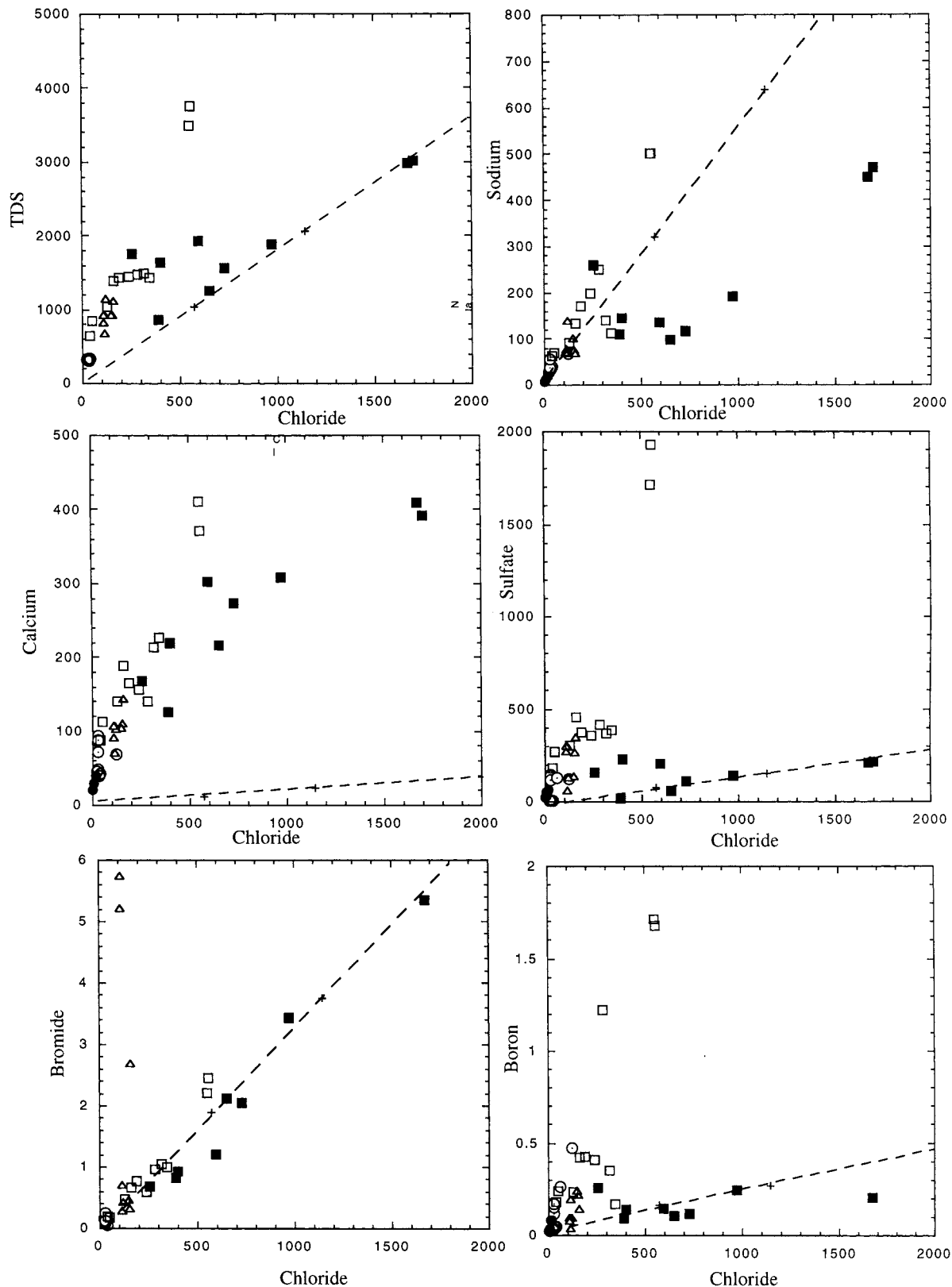


Figure 3. The Chloride versus total dissolved solids (TDS) and other major dissolved salts in groundwater from Salinas Valley as compared to diluted seawater (dashed line). Note the distinction between the different water types (Table 1): fresh groundwater from the northern basin (open circles), surface water (reservoirs and Salinas River) (solid circles), shallow fresh groundwater associated with the Salinas River (circles with a point), high-sulfate nonmarine groundwater from the southern valley and Banana Belt (open squares), groundwater associated with seawater intrusion (solid squares), and high-nitrate groundwater (triangles).

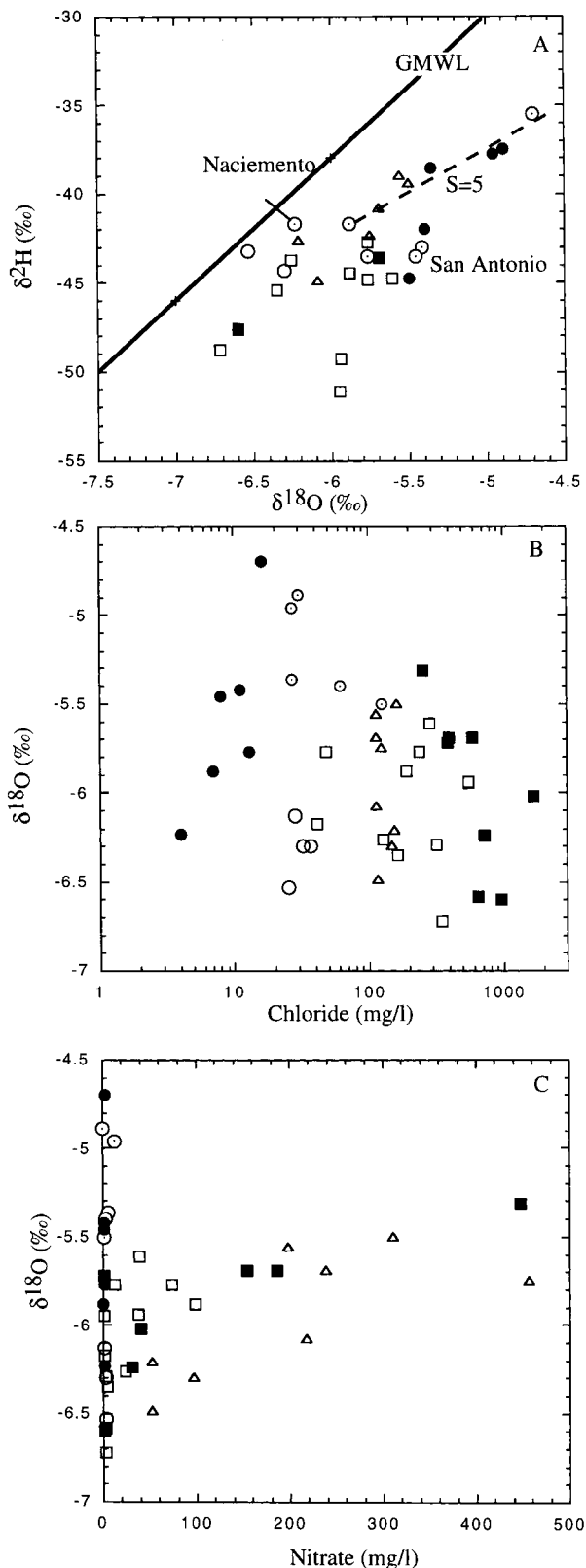


Figure 4. The (a) $\delta^{18}\text{O}$ versus $\delta^2\text{H}$, (b) chloride concentration, and (c) nitrate of the different water groups from Salinas Valley. Symbols for the different water types are as in Figure 3. Note the displacement of most water to the right of the Global Meteoric Water Line (GMWL) due to relatively lower $\delta^{18}\text{O}$ - $\delta^2\text{H}$ slope of surface water and river-associated groundwater that reflects evaporation processes. Also note the positive relationships correlation between $\delta^{18}\text{O}$ and nitrate contents.

The apparent conservative behavior of boron in Salinas Valley groundwater differs from the large isotopic fractionation that occurs in saline water from the Mediterranean coastal aquifer of Israel. Vengosh *et al.* [1994, 1999] showed that the $\delta^{11}\text{B}$ values of groundwater from saltwater intrusion zone are up to +60‰. The high $\delta^{11}\text{B}$ values are associated with low B/Cl ratios (i.e., lower than in seawater, Figure 5) indicating boron removal associated with selective uptake of ^{10}B , probably by sorption onto clay minerals [Vengosh *et al.*, 1994]. The difference may result from different lithology and also from mixing with NO_3 -enriched agriculture return flows with lower $\delta^{11}\text{B}$ (and also $^{87}\text{Sr}/^{86}\text{Sr}$ values, as shown above). Hence mixing of seawater with variable freshwater components adds significant amounts of ^{11}B -depleted boron that is different from the expected two-component mixing values (Figure 5).

4.3. High-Nitrate Waters: Agricultural Return Flow

[25] The Salinas Valley has experienced intensive agriculture activity over the last 5 decades where agricultural irrigation provides about 2 times more groundwater recharge than rainfall annually (Figure 2), resulting in elevated nitrate concentrations in shallow wells (MCWRA, web site). In order to characterize the chemical composition of the agriculture return flow we examined three types of groundwater: (1) shallow groundwater from the perched aquifer (~30 m) below the agriculture fields in the Pressure area (well 14S/2E-11A3), (2) nitrate-enriched groundwater from the unconfined 180-foot aquifer south of Salinas in the East Side subarea, and (3) near-surface groundwater from lysimeters in a strawberry field (Azevedo) at the northwestern end of the valley (Figure 1).

[26] Our results show that shallow groundwater from the perched aquifer (well 11A3) has a distinctive chemical composition with relatively high NO_3 and SO_4 contents (Table 2). The high NO_3 likely reflects the extensive use of nitrogen fertilizers in this area. The high SO_4 probably reflects gypsum fertilizer that is used to enhance permeability and is common in the northern valley where soil is denser (K. Thomasberg, personal communication, MCWRA, 2000).

[27] Groundwater from the perched aquifer has low $^{87}\text{Sr}/^{86}\text{Sr}$ ratios (0.7082) and $\delta^{11}\text{B}$ (+19‰) values, which are associated with a relatively high B/Cl ratio (5×10^{-3}). Therefore both boron and strontium in agriculture return flows may have characteristically low isotopic ratios [e.g., Horan and Böhlke, 1996]. These chemical features are also found in deeper high- NO_3 groundwater from the 180-foot aquifer in the Pressure area. Some saline waters from the "saltwater intrusion" part of this area have high NO_3 concentrations (Table 1), which suggests that they are mixed also with agriculture return flows (see above). These samples also have moderately high SO_4 concentrations in addition to high HCO_3 , relatively low Br/Cl and $\delta^{11}\text{B}$, but high B/Cl values. The low $\delta^{11}\text{B}$ and high B/Cl signature of the agriculture return flow can be attributed to the general enrichment of boron in fertilizers [e.g., Komor, 1997] or, specifically, to boron in gypsum fertilizer as indicated also by the relatively low $^{87}\text{Sr}/^{86}\text{Sr}$ ratios.

[28] In contrast, nitrate-rich groundwater from the unconfined 180-foot aquifer south of Salinas has different chemical and isotopic compositions. They have low SO_4 and B concentrations and high $\delta^{11}\text{B}$ (+31 to +35‰) and $^{87}\text{Sr}/^{86}\text{Sr}$ ratios (0.70895–0.70967) relative to groundwater in the northern Pressure area. The difference implies different recharge sources north and south of Salinas City. Sulfate reduction is an unlikely explanation because this mechanism does not explain the difference in B and Sr isotopic compositions. Instead, we argue that the common use of gypsum fertilizers in the north versus its infrequent use in the south affects the composition of underlying groundwater and that boron and

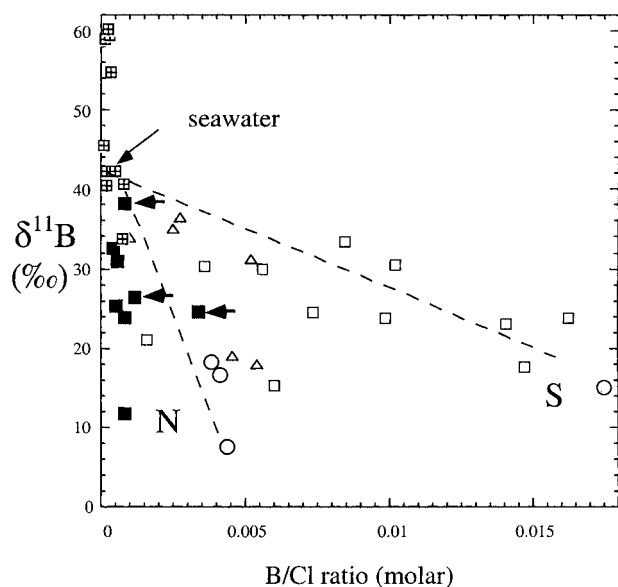


Figure 5. The $\delta^{11}\text{B}$ versus molar B/Cl ratio of different water types from the Salinas Valley (symbols are as in Figure 3) and saline groundwater from the Mediterranean coastal aquifer of Israel (squares with a cross are data from *Vengosh et al.* [1994]). The dashed lines represent possible mixing between seawater and fresh groundwater in the northern basin (N) and river water in the southern valley (S). Alternatively, the lines can represent water-rock interactions accompanied by boron adsorption. In contrast, in the more saline groundwater from Israel the $\delta^{11}\text{B}$ values are higher than that of seawater due to isotopic fractionation associated with extreme boron adsorption; the groundwater associated with seawater intrusion in the Salinas Valley has lower $\delta^{11}\text{B}$ values. Note that the three nitrate-contaminated seawater intrusion samples (marked by arrows) have higher B/Cl ratios reflecting some fertilizer input.

strontium isotopes may be good tracers of anthropogenic sulfate but not always of nitrate contamination.

[29] The positive correlation between high NO_3 groundwater and its $\delta^{18}\text{O}$ (Figure 4c) suggests that the nitrate accumulation in the aquifer is associated with an oxygen isotopic signature of an evaporative surface water source. Similar correlations have been noted for agricultural irrigation water recharge elsewhere in California: the Central Valley [*Davison and Criss*, 1993; *Nascimento et al.*, 1996] and the Ventura basin [*Izbicki*, 1991]. The different relationships between $\delta^{18}\text{O}$ and NO_3 concentrations in surface water versus nitrate-enriched water (Figure 4c and Table 2) enable us to differentiate between the impact of the two principle processes: (1) irrigation that causes evapotranspiration and hence high $\delta^{18}\text{O}$ and NO_3 levels and (2) enhanced recharge via the Salinas River that leads to high $\delta^{18}\text{O}$ and low NO_3 . Further study is required to examine this phenomena in a larger number of groundwater samples.

[30] In addition, the NO_3 -enriched groundwaters are depleted in ^{13}C ($\delta^{13}\text{C} = -23.5$ to -17%) relative to fresh groundwater (-13%), a depletion that appears to vary inversely with calcite saturation (Figure 7). The waters are quite young because of intensive irrigation (see below). Rapidly infiltrating agricultural irrigation water is rich in dissolved CO_2 and is saturated with dissolved oxygen. The accelerated recharge rate compared to natural recharge may contribute to oxidation and mineralization of sedimentary organic matter, which causes the low $\delta^{13}\text{C}$ values

observed in the nitrate-rich groundwater. Note also that the ^{14}C abundance decreases with decreasing $\delta^{13}\text{C}$ for calcite undersaturated groundwater (Figure 7), consistent with an oxidation process of older sedimentary organic matter.

[31] Groundwater impacted by high nitrates and seawater intrusion has lower $\delta^{13}\text{C}$ values than fresh groundwaters. The lower $\delta^{13}\text{C}$ tends to be associated with lower pH values, but all have similar HCO_3 concentrations. Lower pH of the groundwater could result in lower $\delta^{13}\text{C}$ values because the contribution of CO_2 from soil zone increases dissolved carbonic acid with decreasing pH, which has only a small isotopic fractionation with CO_2 gas [*Mook et al.*, 1974]. However, if $\delta^{13}\text{C}$ in soil CO_2 is -25 to -28% , then the low groundwater $\delta^{13}\text{C}$ values cannot be fully explained by low pH. Alternatively, the low $\delta^{13}\text{C}$ may suggest a greater influence of oxidized organic matter (-25 to -28%).

[32] The third site at which we examined the influence of anthropogenic sources is a research strawberry farm where we obtained near-surface (~ 3 m) groundwater from a perched aquifer in Azevedo, northwest of the Salinas River. The site is typical of agricultural areas in California in which methyl bromide has been extensively used for strawberry cultivation. The shallow groundwater has very high nitrate and sulfate concentrations (Table 1), Na/Cl ratio of ~ 1 , extremely high Br/Cl ratios (2×10^{-2}), and low $^{87}\text{Sr}/^{86}\text{Sr}$ ratios (0.7075–0.7076). The high sulfate and the Ca/ SO_4 ratio of ~ 1 suggests the use of gypsum fertilizers. The high Br/Cl ratios may be related to hydrolysis of methyl bromide in the soil that releases inorganic Br to the shallow groundwater. A year prior to the sampling, the fields in the study site had been fumigated (M. Los Huertos, personal communication, 2000). The lower $^{87}\text{Sr}/^{86}\text{Sr}$ ratios are characteristic of the Pajaro River Valley, the next drainage east of the Salinas Valley, which reaches the sea near this site (R. Hanson, U.S. Geological Survey, personal communication, 2000).

4.4. High-Sulfate Water: Nonmarine Water From the Southern Valley

[33] *Bunte and Smith* [1981] and *Showalter et al.* [1984] demonstrated that high-salinity and high-sulfate groundwater is present in the southern Salinas Valley. Surface water from the Diable Range entering the valley from the southeast also contains high sulfate (K. Thomasberg, MCWRA, personal communication, 2001). We sampled two extreme groundwater examples at San Lucas (Figure 1 and Table 1). The groundwater is saline Na- SO_4 type, with conspicuously high ions to chloride ratios relative to the marine ratios (San Lucas wells, Table 2). They also have the lowest $\delta^2\text{H}$ values (Figure 4a) and fall significantly to the right of the Meteoric Water Line compared to other groundwater. This chemical composition differs from that of the seawater intrusion zone or similar types of Ca-chloride brines [e.g., *Vengosh et al.*, 1999]. We therefore do not consider this water as relict brine that evolved from past seawater intrusion that could have been trapped in unflushed or adjacent aquifers. The chemical composition suggests intensive water-rock interactions that resulted in leaching of salts to the liquid phase; the high Na contents can result from weathering of silicate rocks, whereas the high SO_4 can be a result of gypsum dissolution or oxidation of sulfides. Groundwater of nonmeteoric origin is not uncommon in the California Coast Range [*White et al.*, 1973].

[34] The $\delta^{11}\text{B}$ (+24 to 30‰) and $^{87}\text{Sr}/^{86}\text{Sr}$ ratio (0.708524) of the saline water is inconsistent with weathering local silicate rocks which typically have $\delta^{11}\text{B}$ values of ~ 0 to +10‰ and $^{87}\text{Sr}/^{86}\text{Sr}$ of >0.710 . Instead, they indicate sedimentary rocks such as marine gypsum and carbonate which have a $\delta^{11}\text{B}$ range of +20 to +30‰ [*Vengosh et al.*, 1991, 1992]. The Sr isotope ratio may reflect

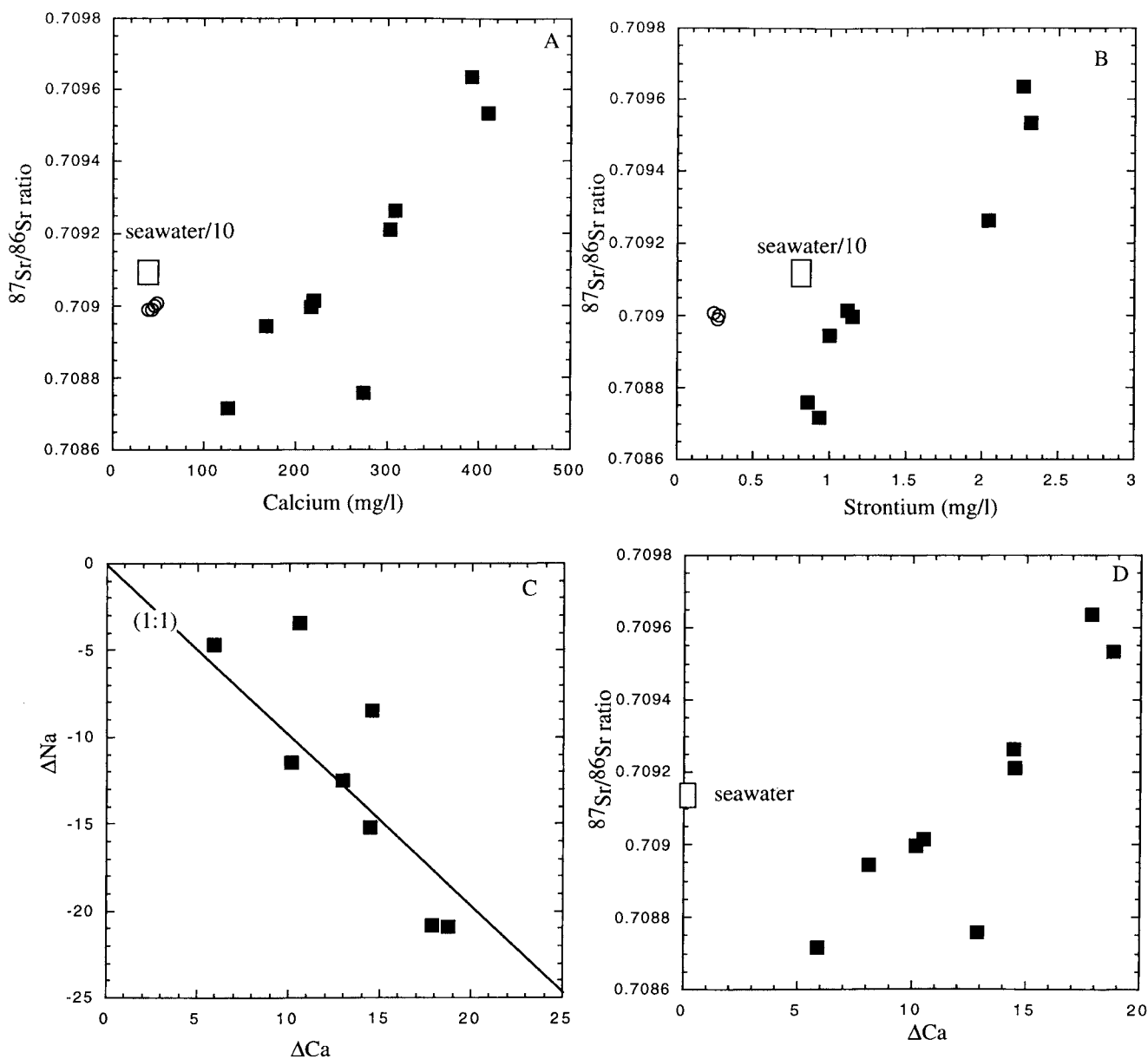


Figure 6. The $^{87}\text{Sr}/^{86}\text{Sr}$ ratio versus (a) calcium and (b) strontium in groundwater associated with seawater intrusion from the Salinas Valley. (c) The ΔCa and ΔNa values. ΔCa is depletion and ΔNa is enrichment of these elements relative to those of diluted seawater with a similar salinity (see text for quantitative definition). (d) The $^{87}\text{Sr}/^{86}\text{Sr}$ values. Note the increase in $^{87}\text{Sr}/^{86}\text{Sr}$ ratios with calcium and strontium concentrations as well as with the relative enrichment of calcium.

dissolution of the Miocene Monterey formation. Unfortunately, the low $^{87}\text{Sr}/^{86}\text{Sr}$ ratio of the high SO_4 natural saline groundwater in the south part of Salinas Valley is indistinguishable from the anthropogenic isotopic signal typical of the Pressure area in the north.

5. Groundwater Ages

[35] A groundwater age determination provides a quantitative means to estimate recharge and subsurface flow rates in groundwater aquifers. For young groundwater (<50 years old), simultaneous measurements of ^3He and tritogenic ^3He in a groundwater sample can be used to calculate a radiometric age, independent of the ^3He source term concentration, by exploiting the parent-

daughter decay relationship [Schlosser *et al.*, 1988]. Accurate tritogenic ^3He measurements entail several correction terms requiring independent measurements of dissolved gases. In short, the tritogenic component of ^3He ($^3\text{He}_{\text{trit}}$) follows the relation

$$^3\text{He}_{\text{trit}} = ^4\text{He}_{\text{air}} \left[\left(\frac{^3\text{He}}{^4\text{He}} \right)_{\text{meas}} - \left(\frac{^3\text{He}}{^4\text{He}} \right)_{\text{air}} \right] + \frac{^4\text{He}_{\text{rad}}}{^4\text{He}_{\text{meas}}}, \quad (2)$$

where the subscript meas refers to measured concentrations and isotopic ratios, subscript air refers to concentration and isotopic ratio of helium isotopes derived from equilibrium and excess air dissolution [Heaton and Vogel, 1981], and subscript rad indicates the radiogenic component of helium derived from uranium-thorium

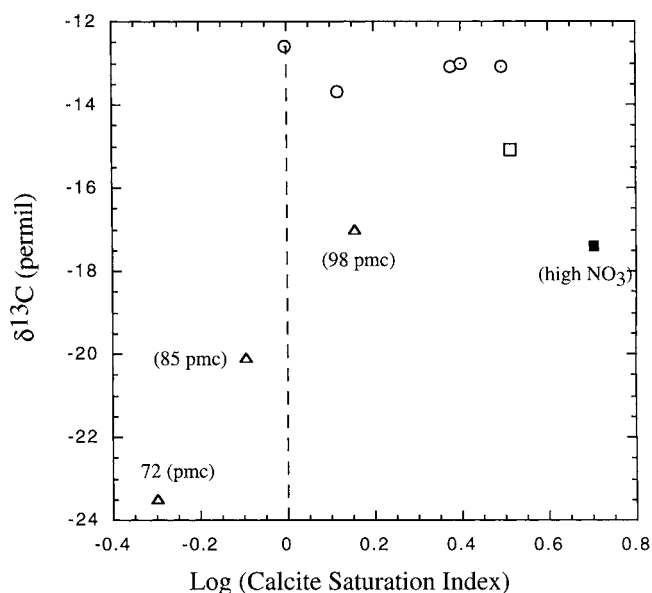


Figure 7. The Calcite saturation index versus $\delta^{13}\text{C}$ of groundwater in Salinas Valley. Symbols are as in Figure 3. Most groundwater in the Salinas Valley is either at or near calcite saturation. However, few samples associated with high- NO_3 groundwater (triangles) show calcite undersaturation, low pH, and low $\delta^{13}\text{C}$ values. A concomitant decrease is associated with $\delta^{13}\text{C}$ and saturation decrease, suggesting a process oxidizing soil organic matter.

decay in the crust [Solomon *et al.*, 1996]. All measurements are reported as concentrations and isotopic ratios relative to laboratory water standards (Table 3). Radiogenic ^3He is assumed to be negligible, and inspection of the ^3He and ^4He concentrations suggests no mantle-derived components in this actively faulted area. The radiogenic ^4He was computed from the difference between measured and expected ^4He concentration, the latter determined from the relationship between dissolved neon and argon concentrations (Figure 8). Relative solubility of argon to neon varies insignificantly over the temperature range in the Salinas Valley, and their covariance due to excess air should be inversely linear. Altitude effects on noble gas concentrations are assumed to be negligible. Note that four groundwaters sampled from the 180-foot aquifer have radiogenic ^4He contributions which plot off the predicted line in Figure 8 and for which calculated correction terms are given in Table 3. The radiogenic ^4He suggests that an older groundwater component may be mixing with younger recharge in these samples [e.g., Mazor and Bosch, 1992]. Although this signal is greatest in a sulfate-enriched sample in the “Banana Belt” area discussed in section 6, the signal is present also in other water types. We attribute its distribution to pockets of older water randomly distributed throughout the basin.

[36] Conversely, widespread young mixing component(s) is indicated by the ^3He – ^3H age results. Tritium concentrations range from 4 to 19 pCi/L, with the lowest concentration in 15S/4E-23M1, which had the highest radiogenic ^4He (Table 3). Tritium concentrations are used to compute the ^3He – ^3H age using the relation

$$\text{age} = 17.9 \ln \left(1 + \frac{^3\text{He}^*}{^3\text{H}} \right), \quad (3)$$

where $^3\text{He}^*$ is the tritiogenic ^3He . Computed ages range from 5 to 38 years before 1997 (Table 3). The oldest age is from well 14S/2E-36E1, the high sulfate groundwater sample noted above, whose

large radiogenic ^3He correction results in an appreciable error in the age estimate (± 10 years). The weak correlation between ^3H concentrations and ^3H – ^3He computed ages indicates that the ^3H is unusually low for all samples even for this coastal environment. For example, ^3H fallout concentration in rainfall from 1963 to 1973 near the coast at Santa Maria, California averaged ~ 550 pCi/L. Furthermore, the youngest groundwater age of 5 years, from fresh meteoric groundwater in the 180-foot aquifer well 14S2E-11A2 in the north, has a ^3H concentration of only 10 pCi/L. In contrast, river recharge groundwater in well 15S/3E-25L1 from the same aquifer in the south has a nearly identical age of 6 years but a ^3H concentration of 17 pCi/L. As a comparison, ^3H concentrations ranging from 15 to 20 pCi/L are commonly observed in undiluted 1-year-old groundwater in southern coastal California [Davisson *et al.*, 1999a, 1999b]. This suggests that young recharge into the Salinas Valley groundwater undergoes appreciable dilution with older nontritiated groundwater in order to produce the observed low ^3H concentrations.

[37] The unusually low ^3H concentrations could also result from crop irrigation using a nontritiated water extracted from deep groundwater sources. Its applicable to the surface and relatively rapid infiltration may lead to incomplete equilibrium with ambient ^3H levels. These return waters could also mix with infiltration from annual precipitation and acquire additional ^3H ; however, precipitation and crop irrigation are normally seasonally offset. Moreover, in the southern Salinas Valley, irrigation water is commonly diverted Salinas River, which would already have ambient ^3H concentrations. Nevertheless, in the northern valley, irrigation water commonly is supplied by groundwater pumping, and incomplete equilibration with ambient ^3H levels during infiltration of return water may explain some of the unusually low ^3H concentrations. Even though different source water could lead to this possible geographic variability in the ^3H input function, the initial ^3H values computed from ^3H – ^3He determinations indicates concentrations are appreciably lower than historical records predict.

[38] In general, ^3H – ^3He ages are ~ 5 years for groundwater from the 180-foot aquifer in the northern valley and 10–20 years for shallow groundwaters apparently recharged from the Salinas River in the south (Table 3). Recharge rates in the Salinas Valley and in the Central Valley of California are high because of extensive agriculture irrigation [Criss and Davisson, 1996]. On the average, in the Salinas Valley, ~ 0.7 m of water is estimated to be applied per hectare each year for irrigation, of which a third is thought to recharge the underlying aquifers (MCWRA, website). Assuming

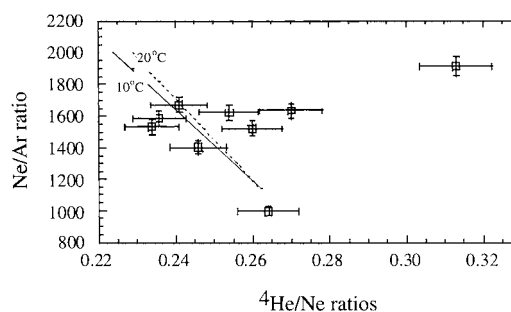


Figure 8. The Ne/Ar versus $^4\text{He}/\text{Ne}$ ratios of groundwater from Salinas Valley. Helium 4 excesses are clearly shown for at least four of the groundwater samples analyzed from the Salinas Valley by their deviation from an equilibrium–excess air mixing line. The radiogenic helium is considered evidence for mixing with older, untritiated groundwater.

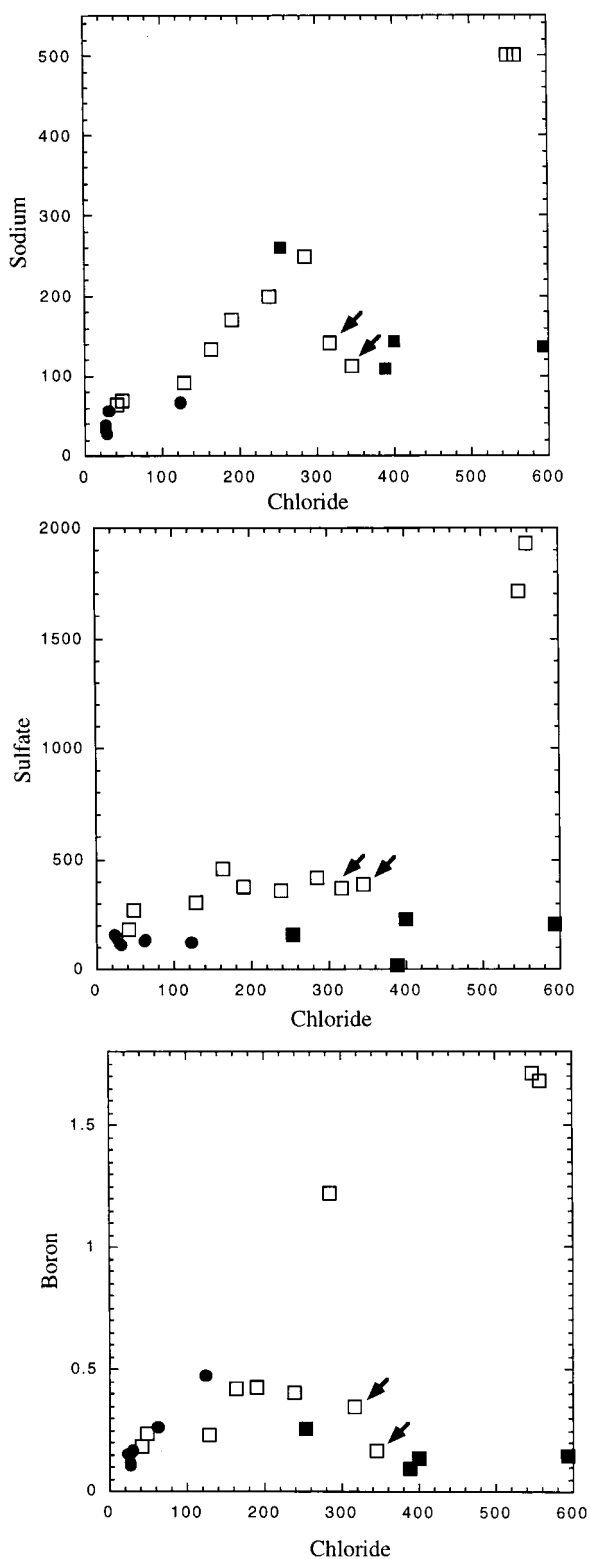


Figure 9. The Chloride versus sodium, sulphate, and boron concentrations in saline groundwater from the southern basin and the “Banana Belt” (open squares), fresh groundwater from the southern basin (circles), and seawater intrusion water (solid squares). The similarity to seawater intrusion of the two Banana Belt samples collected closest to the seawater intrusion front (Figure 1) suggests that they are the earliest stages of seawater intrusion. The four “seawater intrusion” samples lie seaward of the officially recognized front, and three of them have enormously high nitrate due to dilution by agricultural return flows.

piston flow during agricultural recharge and an average aquifer porosity of 25%, a ≤ 1 m/yr recharge to the saturated zone is expected under irrigated areas of the Salinas Valley. Computing general velocities using the ^3H – ^3He ages in Table 3 and aquifer depths in Figure 2 leads to vertical transport rates of 3–10 m/yr. Given the isotopic evidence for mixing between old and young groundwater, the higher suggested recharge rates can be explained by dispersive flow. In addition, mixing of different aquifer depths caused by multiply perforated or long screen intervals in wells cannot be completely ruled out and could lead equally to this effect.

[39] Radiocarbon concentrations were measured for 10 groundwater samples and range from 21 to 103 pmc. The ^{14}C values in all river associated groundwaters exceed 100 pmc, and values in both high-nitrate groundwaters are above 72 pmc. One fresh groundwater from the 400-foot aquifer had 21 pmc indicating an old age, whereas an equally fresh groundwater from the 180-foot aquifer had 77 pmc. The older age from the 400-foot aquifer suggests that current exploitation of this aquifer extracts water without natural balance and replenishment compensation, which makes this aquifer more vulnerable to contamination and overexploitation. In contrast, agricultural irrigation water recharge in the overlying 180-foot aquifer is rapid, as also indicated by the young ^3H – ^3He ages.

6. Mixing of Groundwater Components

[40] Mixing of groundwater components is ubiquitous and reflected in the Salinas Valley in the evidence for randomly distributed pockets of old water with high ^4He and the widespread presence of young shallow tritiated water. Also, the relationships between Cl and other dissolved salts (Figure 3), $\delta^{18}\text{O}$ and Cl and $\delta^{18}\text{O}$ and NO_3 (Figure 4) all reflect mixing of different components. The mixing process is clearly identified using conservative nonreactive tracers (e.g. Cl and $\delta^{18}\text{O}$). In contrast, the variations of reactive elements (e.g. B, Sr, Ca, Na, and C) are additionally affected by water-rock interactions which can be specified qualitatively from the nature of the mixing characteristics observed. This is demonstrated, for example, by the $\delta^{11}\text{B}$ -B/Cl relationship (Figure 5) that demonstrates the mixing of seawater with two different water types (fresh and nonmarine), as well as retention of boron by clay minerals associated with ^{11}B enrichment and overall decrease in elemental boron (e.g. in Israel [Vengosh *et al.*, 1994]). Since most of the groundwater samples were collected from production wells with a large screen length (Table 1), the mixing phenomena are predictable. This situation is typical of many groundwater basins, worldwide, where monitoring research wells are scarce. We argue that the use of geochemical and isotopic tracers enables us to delineate the different groundwater components, even though most of the samples do not represent a final “end-member.”

[41] However, there is at least one coherent region of relatively high-salinity groundwater of ambiguous origin west of Salinas that is characterized by high sulfate but low nitrate (Figure 1). The region is known locally as the “Banana Belt” because of its milder climate. Heard [1992] argued that the high sulfate in this area results from agricultural return flows. However, their relatively high $^{87}\text{Sr}/^{86}\text{Sr}$ ratio (0.7087–0.7100) differs from the low ratios associated with high nitrate agricultural return flow (see section 4.3). In addition, no correlation has been observed between depth of the wells (Table 1) and sulfate concentration.

[42] Selected portions of Figure 3 are shown in expanded scale in Figure 9, in which the open squares are from Banana Belt and are below the 500-mg Cl/L definition for “seawater

intrusion front.” Their locations are shown in Figure 1. All of the waters except the two closest to the “seawater intrusion front” (14S/2E-25D4 and 14S/2E-26PI, identified by arrows in Figure 9) lie on a mixing line between river-associated fresh water and the nonmarine water of the southern valley that we attribute to extensive water-rock interaction. Two samples do not lie on the mixing line and have the highest chloride concentration and low Na. Deviations from simple mixing are even more widespread for sulfate and boron (Figure 9). Moreover, the chemical composition of the most saline groundwater in the Banana Belt is similar to saline groundwater associated with seawater intrusion (solid squares in Figure 9). Consequently, we believe that Banana Belt samples are affected by three principles sources: (1) recent seawater intrusion that extends landward of the 500-mg Cl/L front, (2) lateral flow of nonmarine SO₄-enriched saline water from the south, and (3) fresh recharge that is typical of the southern valley. Water quality measurements from the 1930s and 1940s [Warren *et al.*, 1946] showed that high-SO₄ groundwater already existed in the area at that time.

[43] We suggest that extensive pumping of groundwater, which began in the 1920s, resulted in lowered water levels and formation of a hydrological depression and, consequently, enhanced flow of saline groundwater from the south and development of the seawater intrusion front. Freshwater recharge through the Salinas River has reduced the salinity of the groundwater flowing from the south, particularly in areas where the river is located in the center of the valley (e.g. south of the Banana Belt). This might explain the lack of continuity of salinity in the valley, even though the water level data suggest continuous flow from south to north [Showalter *et al.*, 1984]. A third saline components that is derived from agriculture return flow is identified regionally in the shallow aquifer in some wells that are located north of the seawater intrusion front (wells 14S/2E-11C1, 14S/2E-34N1, and 14S/2E-03F2) but not the within the Banana Belt (Figure 1). This suggest that the Salinas Valley Aquiclude, which confines the 180-foot aquifer in the northern part of the valley (Figure 2), is not uniform throughout the Pressure area. The lack of sealing in some areas resulted in faster arrival of NO₃-enriched agriculture return flow. In other cases, such as the Banana Belt, we suggest that the clay layer provided good protection from return flow but, nonetheless, could not prevent lateral migration of the saline fluids.

7. Conclusions

[44] Traditional investigations of groundwater resources usually utilize geological, hydrological (e.g., water levels), and water quality data in order to establish a conceptual model for the investigated aquifer. Such data are, however, not always fully available. Moreover, in areas of local or international dispute the hydrological data may not be released for a variety of reasons. In order to overcome these obstacles the geochemical approach used in this study provides a “snapshot” observation for the recharge regime, rate of replenishment, sources of salinization, and mixing phenomena in the aquifer. The combined hydrogeological and water quality framework can be used for a conceptual model of the investigated aquifer. It should be emphasized that each of the geochemical and isotopic tracers illuminates different aspects of the hydrological story. Together they provide an integrated picture and further strengthen the reliability of the conceptual model.

[45] Our results provide diagnostic tools that trace the impacts of extensive extraction, irrigation, and soil amendment practices over a complex coastal aquifer system. We show that the chemical and isotopic compositions and age of pristine groundwater are modified as the hydrological balance is changed and external fluids of lesser quality enter the aquifer and mix with fresher recharge. The combination of the hydrogeological structure (e.g., a confining clay layer overlying the aquifer), hydrological balance between extraction and natural replenishment, human activity, and interaction with external saline fluids (e.g., seawater intrusion and nonmarine saline groundwater) determines the level and extent of contamination. Mixing with saline fluids also triggers water-rock interactions such as base exchange reactions, oxidation of organic matter, dissolution of carbonates, sulfate reduction, and nitrification. In particular, we characterize the chemical and isotopic compositions of each of the major components that affect the upper aquifer system of the Salinas Valley as follows (Figure 2):

[46] Natural replenishment in the northern basin is characterized by low dissolved salts, low $\delta^{18}\text{O}$, and rapid recharge to the upper 180-foot aquifer.

[47] Enhanced replenishment from the Nacimiento and San Antonio Reservoirs via the Salinas River in the southern valley is characterized by high $\delta^{18}\text{O}$ and low NO₃/Cl ratios and potentially by high $^{87}\text{Sr}/^{86}\text{Sr}$ ratios.

[48] Seawater intrusion into the northern valley increases the groundwater salinity and is accompanied by base exchanged reaction. As a result, saline groundwater associated with seawater intrusion becomes relatively enriched in Ca and ^{87}Sr and depleted in Na.

[49] Nonmarine saline groundwater flow from south is characterized by relatively high concentrations of total dissolved solids, in particular SO₄ and B relative to Cl.

[50] Agricultural return flow has high concentrations of NO₃ and becomes enriched in ^{18}O (because of evaporation) and depleted in ^{13}C (oxidation of organic matter). Different fertilizer applications can be distinguished by the chemical and isotopic compositions of associated groundwater. In areas where gypsum fertilizers are applied, the contaminated groundwater becomes enriched in SO₄ with low $\delta^{11}\text{B}$ and $^{87}\text{Sr}/^{86}\text{Sr}$ ratios. In areas of methyl bromide fumigation the underlying groundwater is enriched in Br.

[51] Our results also demonstrate the sensitivity of age-dating tools (^3He - ^3H and ^{14}C) to contamination processes. In over-exploited basins, where the original groundwater is extracted and then returned to the aquifer as agriculture return flow, we observe young ^3He - ^3H ages as well as low tritium concentrations and radiogenic ^4He . This reflects rapid arrival of modern recharge mixed with remnants of old groundwater. In contrast, the low ^{14}C values (20 pmc) of groundwater from the deep 400-foot aquifer relative to high ^{14}C values (72–103 pmc) in the upper 180-foot aquifer clearly reflect the nonrenewable nature of deep groundwater, where naturally good water quality is replaced by the poorer quality of modern recharge of the shallow aquifer.

[52] **Acknowledgments.** We thank many staff of the Monterey County Water Resources Agency, especially Kathy Thomasberg and Veronica Ramirez, for assistance in sampling wells, access to GIS and water quality information, and information about regional water topics. Aaron Reyes (UCSC) and Scott Hamlin (USGS) also assisted in the sampling program; Robert Kurkjian and Pete Holden assisted in the TIMS measurements. The USGS provided provisional stable isotope measurements thanks to Randy

Hanson, although all those reported here were made at LLNL. We also thank two anonymous reviewers for their comments. The project was supported by the UC Water Resources Center, grant W-893, and was carried out while A.V. was on sabbatical at UCSC and J.G. was director of the MBEST Center in the Salinas Valley. This work was performed under the auspices of the U.S. Department of Energy by the University of California, Lawrence Livermore National Laboratory under contract W-7405-Eng-48.

References

- Appelo, C. A. J., and D. Postma, *Geochemistry, Groundwater and Pollution*, A. A. Balkema, Brookfield, Vt., 1993.
- Bullen, T. D., A. White, A. Blum, J. Harden, and M. Schultz, Chemical weathering of a soil chronosequence on granitoid alluvium, II, Mineralogical and isotopic constraints on the behavior of strontium, *Geochim. Cosmochim. Acta*, 61, 291–306, 1997.
- Bunte, L. S., and R. R. Smith, Summary of water resources data, report, Monterey County Flood Control and Water Conserv. Dist. Salinas, Calif., 1981.
- Chaudhuri, S., and D. G. Brookins, The Rb-Sr systematics in acid-leached clay minerals, *Chem. Geol.*, 24, 231–242, 1979.
- Chaudhuri, S., V. Broedel, and N. Clauer, Strontium isotopic evolution of oil-field waters from carbonate reservoir rocks in Bindley field, central Kansas, USA, *Geochim. Cosmochim. Acta*, 51, 45–53, 1987.
- Coleman, M. L., T. J. Sheperd, J. J. Durham, J. E. Rouse, and G. R. Moore, Reduction of water with zinc for hydrogen isotope analysis, *Anal. Chem.*, 54, 993–995, 1982.
- Criss, R. E., and M. L. Davisson, Isotopic imaging of surface water/groundwater interactions, Sacramento Valley, California, *J. Hydrol.*, 178, 205–222, 1996.
- Custodio, E., G. A. Bruggeman, and V. Cotecchia, Groundwater problems in coastal areas, *Studies Rep. Hydrol.*, 35, UNESCO, Paris, 1987.
- Davisson, M. L., and R. E. Criss, Stable isotope imaging of a dynamic groundwater system, in the southwestern Sacramento Valley, California (USA), *J. Hydrol.*, 144, 213–246, 1993.
- Davisson, M. L., and R. E. Criss, Stable isotope and groundwater flow dynamics of agricultural irrigation recharge into groundwater resources of the Central Valley, California, paper presented at International Atomic Energy Agency Meeting on Isotope Hydrology, Int. At. Energy Agency, Vienna, March 1995.
- Davisson, M. L., and C. A. Velsko, Rapid extraction of dissolved inorganic carbon from small volumes of natural waters for ^{14}C determination by accelerator mass spectrometry, Lawrence Livermore, Rep. UCRL-JC-119176, 23 pp., Natl. Lab, Livermore, Calif., 1994.
- Davisson, M. L., G. B. Hudson, B. K. Esser, B. Ekwurzel, and R. Herndon, Tracing and age-dating recycled waste water recharge for potable reuse in a seawater injection barrier, southern California, USA, in *Isotope Techniques in Water Resources Development and Management*, Rep. IAEA-SM-361/36, Int. At. Energy Agency, Vienna, 1999a.
- Davisson, M. L., G. B. Hudson, R. Herndon, and G. Woodside, Report on isotope tracer investigations in the forebay of the Orange County groundwater basin: Fiscal years 1996 and 1997, Rep. UCRL-ID-133531, 60 pp. Lawrence Livermore Natl. Lab., Livermore, Calif., 1999b.
- Epstein, S., and T. Mayeda, Variation of ^{18}O content of waters from natural sources, *Geochim. Cosmochim. Acta*, 4, 213–224, 1953.
- Essaid, H. I., USGS SHARP model, in *Seawater Intrusion in Coastal Aquifers—Concepts, Methods and Practices*, edited by J. Bear et al., pp. 213–247, Kluwer Acad., Norwell, Mass., 1999.
- Greene, H. G., Geology of southern Monterey Bay and its relationship to the groundwater basin and salt water intrusion, open file report, 50 pp., Calif. State Dep. of Water Resour., U.S. Geol. Surv., Sacramento, 1970.
- Heard, J. E., Hydrogeology of high-salinity groundwater in the “180-foot” pressure aquifer southwest Salinas, Monterey County, California, M.Sc. thesis, San Jose State Univ., San Jose, Calif., 1992.
- Heaton, T. H. E., and J. C. Vogel, “Excess air” in groundwater, *J. Hydrol.*, 50, 210–216, 1981.
- Horan, M. F., and J. K. Böhlke, Isotopic composition of strontium in agricultural ground waters, Locust Grove, Maryland (abstract), *Eos Trans. AGU*, 77(17), Spring Meet. Suppl. S102, 1996.
- Izbicki, J. A., Chloride sources in a California coastal aquifer, Paper presented at Symposium on Ground Water in the Irrig. Div. Am. Soc. of Consul. Eng., Honolulu, Hawaii, July 22–26 1991.
- Johnson, T. M., and D. J. DePaolo, Interpretation of isotopic data in groundwater-rock systems: Model development and application to Sr isotope data from Yucca Mountain, *Water Resour. Res.*, 30, 1571–1587, 1994.
- Jones, B. F., A. Vengosh, E. Rosenthal, and Y. Yechieli, Geochemical investigations, in *Seawater Intrusion in Coastal Aquifers—Concepts, Methods and Practices*, edited by J. Bear et al., pp. 43–63, Kluwer Acad., Norwell, Mass., 1999.
- Komor, S. C., Boron contents and isotopic compositions of hog manure, selected fertilizers and water in Minnesota, *J. Environ. Qual.*, 26, 1212–1222, 1997.
- Konikow, L. F., and T. E. Rielly, Seawater intrusion in the United States, in *Seawater Intrusion in Coastal Aquifers—Concepts, Methods and Practices*, edited by J. Bear et al., pp. 463–506, Kluwer Acad., Norwell, Mass., 1999.
- Mazor, E., and A. Bosch, Helium as a semi-quantitative tool for groundwater dating in the range of 10^4 – 10^8 years, in *Isotopes of Noble Gases as Tracers in Environmental Studies*, pp. 163–178, Int. At. Energy Agency, Vienna, 1992.
- McNichol, A. P., G. A. Jones, D. L. Hutton, and A. R. Gagnon, The rapid preparation of seawater sigma- CO_2 for radiocarbon analysis at The National Ocean Sciences AMS Facility, *Radiocarbon*, 36, 237–246, 1994.
- Monterey County Water Resources Agency (MCWRA), Hydrogeology and water supply of Salinas Valley, paper presented at Salinas Valley Ground Water Basin Hydrology Conference, Salinas, Calif., June 1995.
- Mook, W. G., J. C. Bommerson, and W. H. Staverman, Carbon isotope fractionation between dissolved bicarbonate and gaseous carbon dioxide, *Earth Planet. Sci. Lett.*, 22, 169–176, 1974.
- Nascimento, C., K. V. Krishnamurthy, and A. Kehew, $\delta^{18}\text{O}$ - δD investigation of surface/groundwater interactions in an agriculture landscape (Abstract), *Eos Trans. AGU*, 77(17), Spring Meet. Suppl., S101–S102, 1996.
- Planert, M., and J. S. Williams, Ground water atlas of United States I, California, Nevada, U.S. Geol. Surv. Hydrol. Invest. Atlas 730-B, 1995.
- Schlosser, P., M. Stute, H. Dorr, C. Sonntag, and O. Munnich, Tritium/ ^3He dating of shallow groundwater, *Earth Planet. Sci. Lett.*, 89, 353–362, 1988.
- Showalter, P., J. P. Akers, and L. A. Swain, Design of a groundwater-quality monitoring network for the Salinas River basin, California, U.S. Geol. Surv. Water Resour. Invest. Rep., 83-4049, 74 pp., 1984.
- Solomon, D. K., A. Hunt, and R. J. Poreda, Source of radiogenic helium-4 in shallow aquifers: Implications of dating young groundwater, *Water Resour. Res.*, 32, 1805–1813, 1996.
- Spivack, A. J., M. R. Palmer, and J. M. Edmond, The sedimentary cycle of the boron isotopes, *Geochim. Cosmochim. Acta*, 51, 1939–1950, 1987.
- Staal, Gardner, and Dunne, Inc., Salinas Valley groundwater basin seawater intrusion delineation/monitoring well construction program, 180-foot aquifer, report, 41 pp., Monterey County Water Resour. Agency, Monterey, Calif., 1993.
- Starinsky, A., M. Bielsky, B. Lazar, G. Steinitz, and M. Raab, Strontium isotope evidence on the history of oilfield brines, Mediterranean Coastal Plain, Israel, *Geochim. Cosmochim. Acta*, 47, 687–695, 1983.
- Stueber, A. M., P. Pushkar, and E. A. Hetherington, A strontium isotopic study of formation waters from Illinois basin, U.S.A., *Appl. Geochem.*, 2, 477–494, 1987.
- Stuiver, M., and H. Polack, Reporting ^{14}C data, *Radiocarbon*, 19, 355–363, 1977.
- Surano, K. A., G. B. Hudson, R. A. Failor, J. M. Sims, R. C. Holland, S. C. MacLean, and J. C. Garrison, Helium-3 mass spectrometry for low-level tritium analysis of environmental samples, *J. Radioanal. Nucl. Chem. Art.*, 161, 443–453, 1992.
- Todd, D. K., Sources of saline intrusion in the 400-foot aquifer, Castroville area, California, report, 41 pp., Monterey County Flood Control and Water Conserv. Dist., Salinas, Calif., 1989.
- Vengosh, A., and I. Pankratov, Chloride/bromide and chloride/fluoride ratios of domestic sewage effluents and associated contaminated ground water, *Ground Water*, 36, 815–824, 1998.
- Vengosh, A., A. R. Chivas, and M. T. McCulloch, Direct determination of boron and chlorine isotopes in geological materials by negative thermal-ionization mass spectrometry, *Chem. Geol.*, 79, 333–343, 1989.
- Vengosh, A., Y. Kolodny, A. Starinsky, A. R. Chivas, and M. T. McCulloch, Coprecipitation and isotopic fractionation of boron in modern biogenic carbonates, *Geochim. Cosmochim. Acta*, 55, 2901–2910, 1991.
- Vengosh, A., A. Starinsky, Y. Kolodny, A. R. Chivas, and M. Raab, Boron isotope variations during fractional evaporation of sea water: New con-

- straints on the marine vs. nonmarine debate, *Geology*, 20, 799–802, 1992.
- Vengosh, A., K. G. Heumann, S. Juraske, and R. Kasher, Boron isotope application for tracing sources of contamination in groundwater, *Environ. Sci. Technol.*, 28, 1968–1974, 1994.
- Vengosh, A., A. J. Spivack, Y. Artzi, and A. Ayalon, Boron, strontium and oxygen isotopic and geochemical constraints for the origin of the salinity in ground water from the Mediterranean coast of Israel, *Water Resour. Res.*, 35, 1877–1894, 1999.
- Vogel, J. S., J. R. Southon, and D. E. Nelson, Catalyst and binder effects in the use of filamentous graphite in AMS, *Nucl. Instrum. Methods Phys. Res.*, B29, 50–56, 1987.
- Warren, E., C. H. Purcell, and E. Hyatt, Salinas basin investigation, summary report, *Bull. 52-B*, Div. of Water Resour. Dep. of Public Works, State of Calif. Sacramento, 1946.
- White, D. E., I. Barnes, and J. R. O'Neil, Thermal and mineral waters of non-meteoritic origin, California Coast Ranges, *Geol. Soc. Am. Bull.*, 80, 935–950, 1973.
-
- M. L. Davisson, Health and Ecological Assessment Division, Lawrence Livermore National Laboratory, L-396, Livermore, California 94550, USA.
- J. Gill, Earth Sciences Department, University of California, Santa Cruz, Santa Cruz, California 95064, USA.
- G. B. Hudson, Analytical and Nuclear Chemistry Division, Lawrence Livermore National Laboratory, L-231, Livermore, California 94550, USA.
- A. Vengosh, Department of Geological and Environmental Sciences, Ben Gurion University of the Negev, P.O. Box 653, Beer Sheva 84105, Israel. (avnerv@bgumail.bgu.ac.il)